INS-17, an insulin-receptor ligand, confers specificity in adult IIS-regulated phenotypes in *C. elegans*

Emily J. Leptich[1,2], Priyadharshini Vijayakumar[2], Edward W. Pietryk[2,3], Meredith I. Williams[2], Rachel N. Arey[2,4*]

[1] Department of Neuroscience, Baylor College of Medicine, Houston, Texas, United States of America

[2] Center for Precision Environmental Health, Baylor College of Medicine, Houston, Texas, United States of America

[3] Department of Molecular and Human Genetics, Baylor College of Medicine, Houston, Texas, United States of America

[4] Department of Molecular and Cellular Biology, Baylor College of Medicine, Houston, Texas, United States of America

*Corresponding author

E-mail: rachel.arey@bcm.edu

Abstract

Insulin/IGF growth factor (IGF) signaling (IIS) is a pleiotropic signaling pathway that functions across tissues to coordinate phenotypic changes in response to nutrient status. Thus, the ubiquity of the IIS pathway hinders efforts to elucidate the mechanisms driving specific IIS-related phenotypes, Previous research in the nematode worm *C. elegans* has demonstrated that loss of function of the IGF transmembrane receptor (IR) ortholog, DAF-2, results in a doubled lifespan and enhanced learning and memory behaviors in young and aged animals. However, these findings are the result of reducing DAF-2 receptor function rather than modulating ligand-receptor interactions. In the current study, we aimed to dissect ligand-receptor interactions that may regulate associative behaviors apart from canonical IIS lifespan phenotypes in *C. elegans*. To this end, we performed targeted genetic screening of Insulin-like Peptides (ILPs) previously identified as DAF-2 antagonists to test their role in learning and memory phenotypes. We discovered that only a single uncharacterized ILP, INS-17, is required for learning and memory. We also demonstrate that INS-17 is sufficient to confer extended memory ability and can promote the maintenance of learning and memory with age. Additionally, we observe that *ins-17* regulates learning and memory ability independent of lifespan, uncoupling IIS-mutant phenotypes. We find that regulation of the *ins-17* genetic locus explains its unique requirement among ILP for learning and memory behaviors. Finally, we found that INS-17 may act to signal a state of nutrient deprivation that is required to properly process stimulus valence to promote advantageous behaviors. Our findings deepen the understanding of how IIS can regulate specific phenotypic outputs in response to changes in internal metabolic states.

Introduction

The survival of most multicellular organisms depends on the coordination of complex physiological processes between multiple, functionally discrete tissues. Remarkably, each of these tissues carries out a diverse set of physiological functions using a highly overlapping set of cell regulatory mechanisms, including ubiquitous signaling pathways (e.g. MAPK/ERK, cAMP, and ubiquitin-proteasome pathway signaling(1–4)). Major components of these pathways are commonly pleiotropic, where a single gene can control multiple, distinct phenotypes depending on the context, such as life stage, cell type, and metabolic state. Across species, one prominent pleiotropic signaling pathway is the insulin/insulin-like growth factor (IGF) receptor signaling (IIS), which regulates a wealth of phenotypes across multiple tissues, including growth and development, metabolism, fertility, aging, stress response, and survival (5–15). Dissecting the specific signaling mechanisms by which IIS mediates such a wide range of phenotypic effects proves challenging, especially in mammalian systems. This is due to several factors, namely high costs to generate tools to examine pathways in a tissue-specific and temporally controlled manner; compensation between receptors, as a single tissue can regulate phenotypes organism-wide; and the time and resource burden to study certain IIS-regulated phenotypes, such as aging. However, invertebrate systems can help overcome these challenges, as IIS is highly conserved across species (9,10,14,16,17), and simple models allow for rapid, low-cost study of genes with remarkable temporal and tissue-specific precision (18–20).

The nematode *C. elegans* has been invaluable in elucidating the pleiotropy underlying IIS phenotypes. In fact, foundational experiments in the worm were the first to link insulin signaling and aging, where loss-of-function receptor mutants of the IR homolog, *daf-2*, have a doubled lifespan of around 40 days compared to the 20-day lifespan of wild-type animals (21,22). Since this initial work, studies in IIS mutants revealed the pleiotropy of the DAF-2 receptor and its conserved downstream signaling components (*age-1*/PI3K and transcription factors *hsf*-1/HSF1, *skn-1*/NRF2, and *daf-16*/forkhead family (FOXO3)) in this relatively simple model (21–28), including that *daf-2* mutants have altered development, metabolism, fertility, motility, cognitive abilities, and more (12,26,29–39). Collectively, research indicates that DAF-2/IR functions across tissues and is integral for sensing internal state along with environmental cues allowing for the worm to adapt appropriately to improve survival.

Despite decades of study of IIS in the worm, how the DAF-2 receptor coordinates a variety of phenotypic responses across tissues remains unclear. This is due in part to the ubiquity of the IIS pathway across tissues, where DAF-2/IR activity in some tissues can mask DAF-2/IR activity in other tissues. For example, it is well established that *daf-2* mutants have improved motility with age (30,40,41), but recent work using degron-based approaches found that reduction of *daf-2* function in neurons and muscles has opposing effects on maintenance of motility in aged animals (42). This work sheds light on the remaining gap in our knowledge regarding how signaling through a single ubiquitous receptor can impact numerous phenotypes that are often reflective of the function of a relatively small number of cells. It is also unclear whether these distinct phenotypes can be uncoupled, and if so by what mechanisms.

87 Though the DAF-2 receptor and its downstream effectors have been well-studied, less is
88 known about the upstream regulators of DAF-2/IR that drive specific phenotypic outputs.
89 The *C. elegans* genome encodes 40 insulin-like peptides (ILPs) predicted to act as DAF-
90 2 receptor agonists or antagonists, sometimes in a context-dependent fashion (43–47).
91 However, no single manipulation of an ILP fully reproduces reduced *daf-2* function
92 phenotypes. ILPs also exhibit diverse and often non-overlapping expression patterns and
93 are regulated by distinct physiological contexts (48). Thus, we hypothesize that pleiotropic
94 phenotypes exhibited by IIS mutants may also reflect distinct ligand-receptor interactions.

95 In the present study, we investigated if specific ILPs regulate *daf-2* mutant learning and
96 memory phenotypes. We discovered that a single ILP, the DAF-2/IR antagonist INS-17,
97 is required for learning and memory ability and is sufficient to promote memory. We also
98 found that INS-17 is specifically required for IIS regulation of behavior and does not
99 appear to be involved in other adult DAF-2 receptor-mediated phenotypes, including
100 lifespan (47,49). We find that the regulation of INS-17 is the source of this phenotypic
101 specificity, and that INS-17 acts as a nutrient-deprivation signal that regulates plastic
102 behavior in the context of changing physiological states.

103 Results

104 INS-17 is specifically required for learning and memory ability

105 Decreased DAF-2 receptor function results in a 3-fold extension in short- and intermediate
106 associative memory (S/ITAM), as measured by positive olfactory association assays (31).
107 In this paradigm, animals form a positive association with the neutral odor butanone (10%
108 in EtOH) when paired with food, which is measured by a training-dependent increase in

109 butanone chemotaxis (50). A single food-butanone (1 CS-US) pairing usually results in a
110 molecularly conserved memory that lasts approximately 2 hours; however, young adult
111 *daf-2* mutants maintain a food-butanone association for up to 6 hours (Fig. 1A) (31).
112 Percent maximum (% Max) performance indices are shown for clarity (see methods for
113 calculations), as *daf-2* animals have high naïve chemotaxis to 10% butanone in multiple
114 studies (31,34,36,37) (Fig. S1A) that contribute to perceived learning impairments when
115 graphed with raw performance indices (provided in Fig. S1B). Given that partial loss-of-
116 function *daf-2* animals display this significant extension in S/ITAM performance, we
117 hypothesized that insulin receptor antagonist(s), which are predicted to reduce signaling
118 through DAF-2/IR, may promote learning and memory behavior (Fig. 1B). To test this
119 hypothesis, we examined the learning and memory ability of publicly available insulin
120 receptor antagonist mutants using this STAM paradigm. We tested learning and
121 intermediate-term associative memory (ITAM, 60 minutes post-training), as behavioral
122 deficits are typically more prominent at this timepoint compared to STAM (30 minutes
123 post-training). Mutants tested included predicted strong (*ins -17, -37, and -39)* and weak
124 (*ins-15, -21,* and *-22)* antagonists (47,51,52). However, we recently determined that
125 mutants for *ins-22* have an abnormally high preference for 10% butanone (Fig. S1I) (53).
126 Thus, we excluded *ins-22* from our targeted behavioral screen, as this high naïve
127 chemotaxis would make it difficult to measure training-dependent increases in butanone
128 preference. Most antagonist mutants behaved in a manner that was indistinguishable
129 from wild-type animals, including baseline naïve chemotaxis (Fig. 1D-E, S1E-H); while
130 mutant animals for *ins-39* had significantly higher intermediate-term associative memory
131 (ITAM) performance compared to wild-type animals, we were screening for behavioral

132 deficits and focused on candidates that had impaired behavioral performance.
133 Interestingly, only loss-of-function mutants of *ins-17* exhibited behavioral deficits: these
134 include significant deficits in learning, STAM and ITAM performance (Fig 1C). These
135 deficits were not accompanied by impaired sensory function, as measured by naïve
136 chemotaxis assays to the highly attractive concentration (0.1%) of butanone (Fig. S1C-
137 D), suggesting that they are specific to learning and memory. INS-17 is a relatively
138 uncharacterized ILP; aside from its prediction as a strong antagonist, previous research
139 has established *ins-17*'s role in regulating dauer formation in early development (49). To
140 our knowledge, INS-17 is uncharacterized regarding complex behavior, and these results
141 (Fig. 1C-E) suggest that it is a novel learning and memory-regulating ILP.

142 INS-17 signals through DAF-2 and promotes memory

143 We next wanted to confirm that INS-17 signaling was indeed mediated by the DAF-2
144 receptor and tested the learning and memory behavior of *daf-2(e1370);ins-17(tm790)*
145 double mutants. We examined double mutant memory behavior at 3 hours after 1x
146 training, a timepoint where *daf-2* mutants exhibit extended memory (31). *daf-*
147 *2(e1370);ins-17(tm790)* worms demonstrated extended 3-hour memory indistinguishable
148 from *daf-2* animals (Fig. 2A, S2A-C). Thus, we infer from these results that DAF-2/IR is
149 epistatic to INS-17 in the regulation of learning and memory.

150 Next, we wanted to explore how manipulating levels of INS-17 may influence behavioral
151 outputs. Our behavior paradigm tests an adult-specific behavior (34), and *ins-17* regulates
152 dauer in development (49), so we sought to avoid confounding our results with
153 developmental effects of traditional transgenic approaches. Recently, we developed a
154 novel microbial feeding paradigm to manipulate neuropeptide signaling specifically in

155 adult animals (53). In these experiments, *C. elegans* are fed *E. coli* bacteria expressing
156 a plasmid containing the sequence encoding a neuropeptide of interest flanked by
157 processing enzyme cut sites (Fig. 2B). Like feeding-based RNAi approaches (54), this
158 method offers precise temporal control of increasing neuropeptide levels via adult-only
159 manipulation to avoid potential effects on early development. We have demonstrated that
160 this feeding method could work in an 'overexpression' manner when administered to wild-
161 type animals, altering sensory behavior (53). Here, we wanted to extend this approach to
162 assess if administering additional INS-17 to adult animals could affect associative
163 behaviors. We hypothesized that increasing the levels of a memory-regulating *daf-2*
164 antagonist would result in enhanced memory ability. Briefly, we fed L4 animals *E. coli*
165 expressing either INS-17 or a scrambled control peptide (SCR) and examined their
166 behavior at Day 2 of adulthood.

167 To first establish the ability of this method to effectively manipulate INS-17 signaling, we
168 tested if INS-17 peptide feeding was sufficient to rescue learning and memory behavior
169 of *ins-17(tm790)* animals. SCR fed mutants still exhibited behavioral deficits, while adult-
170 only feeding of INS-17 to *ins-17* deficient mutants was sufficient to rescue their behavior,
171 similar to wild-type animals fed SCR peptide (Fig. 2C). Notably, we determined these
172 results were not the result of sensory deficits in these animals (Fig. S2D-E). We next
173 explored if INS-17 peptide feeding was sufficient to boost wild-type animal memory
174 behavior past the 2-hour timepoint after 1x training. Remarkably, we found that wild-type
175 animals fed INS-17 during adulthood displayed 3-hour memory post-training, while SCR
176 fed animals demonstrated no memory phenotype, as expected (Fig. 2D). We confirmed
177 that peptide feeding to both wild-type and mutant animals did not alter baseline

178 chemosensation, indicating the effect is memory-specific (Fig. S2D-F). These results
179 suggest that increasing INS-17 is sufficient to boost cognitive performance and
180 phenocopy *daf-2* animals' 3-hour memory behavior.

181 Finally, we worked to identify the tissue where INS-17 is required to regulate memory.
182 Since INS-17 is highly expressed in the nervous-system, we hypothesized that neurons
183 may use INS-17 as a memory signal. Using a neuron-specific RNAi-sensitive line(55), we
184 performed an adult-only *ins-17* knockdown and observed significant S/IATM behavioral
185 deficits in *ins-17 RNAi* knock-down animals (Fig. 2E)—similar to what we observed in
186 deletion mutants (Fig. 1B)—with no detectable effects on sensory ability (Fig. S2H-I). This
187 demonstrates that INS-17 is a memory-promoting DAF-2/IR antagonist, likely released
188 from neurons.

189 INS-17 regulates the cognitive aging phenotypes mediated by 190 the DAF-2 receptor independent of lifespan

191 In addition to exhibiting extended STAM at young adult stages, *daf-2* mutants also
192 maintain the ability to learn and remember after 1 CS-US pairing with age (31). Wild-type
193 animals display age-related cognitive deficits as early as Days 3 and 5 of adulthood (Fig
194 3A-B, S3A-C), while *daf-2* mutants maintain performance akin to Day 1 of adulthood at
195 these timepoints. Therefore, we wanted to ask if INS-17 could also be involved in these
196 age-related phenotypes associated with altered *daf-2* function. As *ins-17* mutants already
197 display severe behavioral defects at Day 1 of adulthood, we examined the effect of
198 increased INS-17 on age-related behavioral impairments in wild-type animals, again
199 using a peptide feeding-based approach (53).

200 We first assessed the behavior of animals supplemented continuously with INS-17 from
201 the L4 stage until Day 5 of adulthood (Fig. 3C), when worms are considered cognitively
202 aged (31). INS-17 fed animals demonstrated significantly better learning and memory
203 performance compared to wild-type SCR fed controls (Fig. 3C-D, S3D). Next, we
204 wondered if manipulating the DAF-2/IR pathway via INS-17 later in life could influence
205 cognitive aging, as previous work has shown that degradation of DAF-2/IR via an auxin
206 inducible degron system in older animals results in improved STAM (37). We subjected
207 Day 3 adult wild-type animals (which already display age-related cognitive deficits
208 compared to Day 1 Adults (Fig. 3A)) to SCR or INS-17 peptide feeding and tested their
209 learning and memory abilities at Day 5 of adulthood (Fig. 3E). Notably, we found that Day
210 5 INS-17 fed animals had better learning and STAM behaviors compared to SCR fed
211 controls (Fig. 3E-F, S3E-F). These findings suggest that INS-17 is a DAF-2/IR ligand that
212 could partially contribute to the enhanced cognitive ability with age observed when DAF-
213 2/IR activity levels are reduced.

214 Since *daf-2* animals have both a doubled lifespan and enhanced memory phenotypes in
215 young and aged animals (21,31), we wanted to determine if manipulating INS-17*,* as a
216 strong DAF-2/IR antagonist, would alter lifespan in addition to associative behaviors. As
217 previously reported in the literature (49), we confirmed that *ins-17(tm790)* animals have
218 no significant difference in lifespan to wild-type animals (Fig. 3G, S3F-G). We also tested
219 the lifespans of wild-type animals fed SCR compared to those fed INS-17 in adulthood,
220 finding no significant differences between groups (Fig. 3H, S3H-I). Thus, our findings
221 demonstrate that either loss of *ins-17* or increased levels of INS-17 has no effect on adult

222 lifespan, highlighting the specific phenotypic regulation by individual ligands underlying
223 the pleiotropy of the DAF-2 receptor.

224 INS-17 engages multiple pathways downstream of DAF-2 to 225 regulate learning and memory

226 We next sought to identify the pathways downstream of DAF-2/IR that could explain the
227 phenotypic specificity of INS-17. The canonical downstream target of DAF-2/IR signaling
228 is the FOXO transcription factor homolog DAF-16(27,28), which is required for the
229 doubled lifespan extension of *daf-2* loss-of-function worms (26,28,56). Additionally, *daf-*
230 *16* mutants exhibit severely impaired learning and memory phenotypes (Fig. 4A, S4A
231 (31). Since *ins-17* is required for positive associative memory behavior and there are no
232 adult lifespan phenotypes associated with *ins-17* (Fig 3G-H), we hypothesized that *ins-*
233 *17* activates a pathway that acts in parallel to *daf-16*. To test this, we examined if INS-17
234 feeding could improve the memory impairments of *daf-16* worms. We found that adult-
235 only INS-17 feeding rescued the learning and memory of *daf-16(mu86)* animals to SCR
236 fed wild-type performance levels, while SCR fed *daf-16(mu86)* worms still displayed
237 behavioral deficits (Fig. 4B, S4B-C). These results support that INS-17 could act
238 independently of DAF-16 to regulate associative behaviors.

239 Regulation of the *ins-17* genetic locus is required for proper 240 regulation of behavior

241 While we had identified how INS-17 might regulate distinct DAF-2/IR mediated
242 phenotypes, we also sought to examine what made INS-17 unique relative to other

243 antagonists in regard to regulating behavior. Interestingly, though the *C. elegans* genome
244 encodes 40 ILPs, there are only three structurally similar antagonists known as γ-insulins;
245 these genes are encoded across multiple genomic regions (ch. II and III) and thus likely
246 under the control of distinct regulatory elements (43,47,57). We therefore hypothesized
247 that phenotypic specificity was not necessarily due to insulin class or structure, but
248 instead via *ins-17*'s regulation by its surrounding genomic elements, which likely respond
249 to different signaling pathways and environmental cues. To test this hypothesis, we
250 explored if replacing *ins-17* with another strong DAF-2/IR antagonist was sufficient to
251 maintain normal positive associative memory ability in an *ins-17* mutant background.

252 We selected *ins-37* to swap in for *ins-17* due to a key overlap in structure, as both ILPs
253 are predicted strong DAF-2/IR antagonists and are γ-insulins, which are defined by three
254 di-sulfide bonds (47). Moreover, *ins-37* mutants had no observable learning and memory
255 impairments (Fig. 1D, S1H) and *ins-37* is lowly expressed in neurons (58), making it an
256 ideal strong antagonist to test our hypothesis. Thus, we generated an *ins-17* CRISPR
257 knockout in which we placed the *ins-37* coding sequence at the *ins-17* locus (Fig. 5A).
258 Subsequently, we examined if *ins-37* expressed at endogenous *ins-17* levels is sufficient
259 for normal learning and memory behavior. First, we confirmed that the newly generated
260 *ins-17* knockout line exhibited learning and memory impairments similar to the predicted
261 loss-of-function mutants (Fig 1C, 5B, S5A). Interestingly, we found that replacing *ins-17*
262 with *ins-37* could rescue the defective learning and memory of *ins-17* KO animals,
263 functionally replacing endogenous *ins-17* (Fig. 5B, S5A). These results indicate that ILP
264 structure is not as critical as its regulation of expression. These results suggest that the

genomic context in which *ins-17* is regulated underlies its importance in promoting specific behavioral phenotypes.

ins-17 expression rapidly responds to nutrient deprivation

Next, we wanted to uncover the physiological conditions that regulate *ins-17* expression and assess their role in learning and memory. We mined publicly available gene expression datasets and discovered that *ins-17* transcription is likely regulated by metabolic state, as it is consistently upregulated in multiple starvation paradigms and genetic models of nutrient deprivation (Table 1) (49,51,59–62). Interestingly, our appetitive behavioral paradigm involves a 1-hour food deprivation (FD) step prior to the 1 CS-US (food-butanone) pairing, which has been reported to promote a more robust CS-US association compared to animals that do not undergo a FD period prior to memory training (31,63). We first examined if the FD step incorporated into our paradigm was sufficient to increase *ins-17*. We performed qPCR analysis to measure *ins-17* levels in wild-type worms after 1 hour of FD and found that even this short time period was sufficient to observe a significant increase in *ins-17* expression (Fig. 5C, left). We also observed more robust upregulation of *ins-17* following 2 hours of FD (Fig. S5B), suggesting that this locus rapidly responds to changes in nutrient availability.

INS-17 is required for properly sensing internal nutrient status to allow for processing of stimulus valence

Based on our gene expression results, we hypothesized that INS-17 could promote memory performance by functioning as a FD signal. We first assessed the role of insulin

286 signaling in FD-associated improvements in associative behavior (Fig. 5C, right). We
287 confirmed that FD could indeed improve memory ability by comparing the behavioral
288 performance of wild-type animals that underwent FD prior to training to animals that were
289 not food-deprived (non-FD) prior to training. Similar to previous reports (31), we found
290 that wild-type FD animals have significantly better ITAM performance, which is measured
291 one hour post-training, compared to non-FD animals (Fig. 5D, S5C-D). Interestingly, *daf-*
292 *2* mutant phenotypes are strongly associated with phenotypes paralleling those of
293 chronically starved worms (64–67), so we hypothesized that *daf-2* animals may not
294 require the FD step prior to 1 CS-US pairing for robust ITAM behavior, as they are thought
295 to have a perceived nutrient status of chronic starvation even when well-fed. We found
296 that non-FD *daf-2* animals that underwent 1 CS-US pairing had ITAM behavior nearly
297 identical to *daf-2* animals that were FD prior to training (Fig. 5E, S5E). Altogether, these
298 results indicate that *daf-2* animals' improved memory phenotype could be driven by their
299 sensation of a chronically starved internal state.

300 We next tested if INS-17 could function as a FD signal. If this was the case, we
301 hypothesized that increased levels of INS-17 could be sufficient to promote robust ITAM
302 behavior in the absence of the FD step prior to 1 CS-US pairing. To test this, we examined
303 if wild-type animals fed INS-17 peptide required FD for enhanced ITAM. We compared
304 memory performance of SCR or INS-17 fed animals after training in the absence of FD,
305 and found that, similar to *daf-2* mutants, INS-17 fed animals exhibited significantly more
306 robust ITAM than SCR fed animals in the non-FD condition (Fig. 5F). Furthermore, FD
307 had no detectable effect on ITAM performance in INS-17 fed animals, but significantly

308 improved ITAM in SCR fed animals (Fig. S5F-I). These results suggest that INS-17 acts
309 as a FD signal to promote a stronger association between a food and an odorant.

310 We next asked if INS-17 functions generally as a FD signal to promote associative
311 behaviors using an aversive olfactory training paradigm, where an attractive odorant
312 diacetyl is paired with the absence of food to form a negative association (68). If INS-17
313 functions as a signal of FD internal state, we hypothesized that *ins-17* mutants would
314 have impaired aversive learning and memory compared to wild-type animals, because
315 sensing starvation is required for a negative diacetyl association to be formed. Wild-type
316 and *ins-17* loss-of-function mutants underwent well-established aversive memory assays
317 using a diacetyl-starvation pairing (68). Strikingly, we found that *ins-17* is required for
318 normal aversive associative behaviors, as *ins-17* animals had severe deficits in learning,
319 STAM, and ITAM behavior compared to wild-type animals (Fig. 5G, S5J). The aversive
320 and appetitive olfactory conditioning paradigms we tested here recruit distinct neuronal
321 circuits (63,69–75). Therefore, our results suggest that *ins-17* may be broadly required in
322 the nervous system to signal a FD state so that the valence of olfactory stimuli (positive
323 when paired with food, negative when paired with starvation) can be processed
324 appropriately to promote advantageous behaviors (Fig. 5H). This could explain how IIS
325 acts in the nervous system to integrate metabolic status and regulate specific behavioral
326 outputs, such as learning and memory.

327 Discussion

328 Across species, insulin signaling is pleiotropic. In the worm, the DAF-2 receptor regulates
329 a wide array of phenotypes, including those related to development, lifespan, metabolism,

330 fecundity, cognitive behaviors, and motility, among others. How does a single receptor
331 mediate such physiologically distinct phenotypes? Here we report that some of these
332 pleiotropic actions result from specific ligand-receptor interactions. In this instance, we
333 show that an olfactory memory phenotype is likely mediated by INS-17, an antagonistic
334 ILP with no previously reported role in behavior (to our knowledge). DAF-2 receptor partial
335 loss-of-function mutants have a well-established extended memory phenotype (31), so it
336 is not surprising that a predicted antagonistic ILP regulated these behaviors. However,
337 we were surprised that only a single strong antagonist appeared to be required in our
338 paradigms. The importance of INS-17 to the extended memory phenotype is supported
339 by our finding that overexpression through feeding is sufficient to recapitulate the memory
340 phenotype of *daf-2* mutants. While we established that other antagonists are not required
341 for this specific behavioral phenotype, many ILPs are diverse and act as agonists or
342 antagonists in a context-dependent fashion, and most do not have a described role in
343 associative behaviors. Future studies systemically characterizing these diverse ligands
344 will be informative for defining DAF-2 receptor pleiotropy across tissues.

345 Interestingly, several transcriptomic datasets show that *ins-17* transcripts are increased
346 roughly 2-fold in *daf-2* mutants and decreased in *daf-16* mutants compared to wild-type
347 animals (Table 1) (34,49,51,59,60,62). This indicates that INS-17 is highly regulated by
348 IIS signaling and is potentially acting both upstream and down-stream of DAF-2/IR. “ILP
349 to ILP” signaling, where the action of one ILP affects the expression of another ILP, could
350 be a component of *ins-17*’s role in integrating sensory cues and nutrient availability to
351 elicit behavioral outputs. One example of “ILP to ILP” signaling in behavior is between
352 INS-6 and INS-7 in aversive pathogen learning, where INS-6 released by the ASI neuron

353 regulates *ins-7* transcription in the URX neurons to regulate this behavior (76). Further
354 transcriptional analysis of *ins-17* mutants and INS-17 overexpression models could
355 provide insight into which ILPs may be regulating or be regulated by INS-17.

356 We also report that INS-17's function in adulthood is specific to behavior, as manipulating
357 INS-17 does not affect lifespan (49). While *daf-2* animals' extended lifespan is a canonical
358 phenotype, there may exist alternate downstream IIS pathways that are dispensable for
359 lifespan regulation. There are reports that the sole insulin receptor substrate homolog
360 IST-1 may differentially activate distinct arms of the IIS signaling pathway, as it can
361 function upstream of—or partially in parallel to—DAF-16 and is not required for normal
362 growth and development (77–79). Thus, it is possible the 40 known ILPs may similarly
363 engage the IIS pathway. In the present study, we investigated IST-1, which engages
364 atypical IIS signaling to regulate aversive olfactory learning (79). Here, we report that *ist-*
365 *1* mutants display positive olfactory memory deficits that were rescued by INS-17 peptide
366 feeding; taken with our similar results in *daf-16* mutants, these findings suggest INS-17
367 may activate multiple arms of the IIS pathway to regulate adult cognitive behaviors. We
368 find that *daf-16;ist-1* double mutants do not respond to INS-17 peptide supplementation,
369 suggesting that, similar to other olfactory behavioral paradigms(79), INS-17 engages
370 multiple pathways that can act partially in parallel to one another downstream of DAF-2
371 to regulate behavior. It will be intriguing in the future to examine if other DAF-2-mediated
372 associative behaviors similarly engage both downstream pathways.

373 We also find that the genomic context in which an ILP is regulated provides specificity, as
374 "swapping" a structurally similar insulin, *ins-37* (47), into *the ins-17* genetic locus is
375 sufficient to functionally replace *ins-17* in behavior, though endogenous *ins-37* is not

376 required for learning phenotypes in our paradigm. This result supports that tissue-specific
377 gene regulation may inform DAF-2/IR pleiotropy, warranting future studies exploring
378 tissue-specific requirements for DAF-2/IR function.

379 Furthermore, we demonstrate that *ins-17* is required for both positive and aversive
380 associative behaviors. Both associative behavioral paradigms include a relatively short,
381 1-hour FD step prior to training to prime animals to form a stronger association between
382 food and an odorant, thus promoting a more robust behavioral response after training.
383 This FD step occurs within the timeframe before animals display significant changes in
384 sensory integration behavior due to a “lack of food sensation”, which begins after 3 hours
385 of food-deprivation (80); however, food is cleared from the alimentary system within 2
386 minutes of ingestion (81,82), suggesting the need for a FD signal to inform robust
387 behavioral responses after only 1 hour of FD. Our gene expression data, similar to
388 previous studies (51,59,60), shows that the *ins-17* gene is activated in this timeframe,
389 suggesting that could it be involved in responding to these brief FD signals. This notion is
390 supported by our findings that feeding INS-17 to animals that do not undergo FD results
391 in normal learning and memory, bypassing the need for FD to promote memory. Together,
392 these results suggest that INS-17 could be released in response to acute and prolonged
393 FD to inform sensory integration behavior. Interestingly, the only phenotype previously
394 associated with INS-17 is dauer formation to protect progeny from unfavorable conditions
395 (49), namely starvation (83). We speculate that INS-17 may respond to FD to coordinate
396 phenotypic responses in different life stages that are most advantageous; for example,
397 while *ins-17* regulates dauer formation, which is a response to lack of food availability and
398 other stresses during development, it may also regulate the ability to form associations in

399 the context of food availability in adulthood, which is beneficial for egg-laying and progeny
400 survival (64,84). In the future, it will be interesting to further examine how both the *ins-17*
401 locus and INS-17 secretion are regulated in the context of changing nutrient availability.

402 Since *ins-17* is required for both positive and aversive associative behaviors, our results
403 support that INS-17 may function as a broad signal for nutrient deprivation to the nervous
404 system. *ins-17* is widely expressed across the nervous system (58,61), but is most highly
405 expressed in the AIZ interneuron, which mediates a variety of behavioral outputs in
406 response to multiple sensory neurons and circuits (85–87). We observed that associative
407 behavior impairments resulting from loss of ins-17 do not stem from baseline sensory
408 deficits, which strongly indicates that rather sensory information may not be integrated
409 correctly or that sensory neurons cannot alter their responses to an environmental
410 stimulus in the context of altered metabolic status. We have established that INS-17 may
411 be essential for interpreting internal state and proper valence processing. In mammals,
412 neuropeptides also are important for signaling valence in positive and aversive
413 associative paradigms (88,89), and this is likely a theme of peptides modulating circuits
414 more broadly. Future studies examining how INS-17 regulates sensory circuit activity in
415 various contexts will help further define *daf-2* pleiotropic mechanisms.

416 Our results bring an attractive model for the expansion of the ILP family in *C. elegans*.
417 ILPs are encoded across the genome and function under the control of a variety of
418 regulatory elements so the animal can dynamically respond to a combination of nutrients
419 and environmental stimuli via DAF-2/IR to facilitate the most advantageous phenotype.
420 Having a diverse array of peptides that can carry out distinct outputs is beneficial,
421 especially if there is only one receptor to mediate such outputs. In the case of INS-17,

422 being able to properly make associations in the face of changing environments can
423 promote survival, such as remembering availability (or lack) of a food source associated
424 with specific odors. Together, our findings have identified INS-17 as a physiological signal
425 that is required for positive and aversive associative behaviors and may integrate
426 environmental cues and nutrient status to inform valence processing and regulate
427 behavioral outcomes. This research underscores the importance of future work
428 investigating the rich and diverse network of DAF-2/IR signaling.

429 Methods

430 General *C. elegans* maintenance

431 Worms were maintained at 20 °C on plates containing either 1) Standard nematode
432 growth medium (NGM): 3 g/L NaCl, 17 g/L agar, 2.5 g/L peptone, 25 mL/L KPO4 (pH
433 6.0), 1 mL/L MgSO4, 1 mL/L CaCl2, and 1 mL/L cholesterol (5 mg/mL in ethanol) (90); or
434 2) High growth medium (HGM): 3 g/L NaCl, 30 g/L agar, 20 g/L peptone, 25 mL/L KPO4
435 (pH 6.0), 1 mL/L MgSO4, 1 mL/L CaCl2, and 4 mL/L cholesterol (5 mg/mL in ethanol)
436 (50). Plates were seeded with an *E. coli* OP50 lawn for ad libitum feeding (90).

437 Animals were developmentally synchronized using an alkaline-bleach solution (1.5 mL 5
438 N NaOH, 3.0 mL 5% sodium hypochlorite, 5.5 mL water) to collect eggs from gravid
439 adults; eggs were subsequently washed three times with M9 buffer solution (6 g/L
440 Na2HPO4, 3 g/L KH2PO4, 5 g/L NaCl and 1 mL/L 1M MgSO4 in ultrapure water) before
441 plating (90).

442 Strains

443 Wild-type: N2 Bristol

444 Mutants: *ins-17(tm790), ins-21(tm5180)*, *ins-37(tm6892)*, and *ins-39(tm6520)* were
445 obtained from the National BioResource Project, Japan.

446 RB2489 (*ins-15(ok3444)*), RB2594 (*ins-22(ok3616)*), CB1370 (*daf-2(e1370)*), CF1038
447 (*daf-16(mu86)*), MAH677 (*sid-1(qt9) V; sqIs71[rgef-2p::GFP + rgef-1p::sid-1]*) were
448 obtained from the Caenorhabditis Genetics Center.

449 CX17790 (*ist-1(ok2706)* was described previously(79) and generously gifted to us by
450 Dr. Cornelia Bargmann.

451 Strains made in collaboration with InVivo Biosystems include *ins-17* CRISPR KO
452 animals with *ins-37* replacement COP2848 (*ins-17(knu1330[ins-37]) III*) and *ins-17*
453 CRISPR KO animals COP2835 (*ins-17(knu1320) III*).

454 The following strains were generated by crosses: RNA34 (*daf-2(e1370)*; *ins-17(tm790))*
455 and RNA59 (*daf-16(mu86); ist-1(ok2706)*).

456 Peptide plasmid generation and transformation

457 The amino acid coding sequence for each peptide was identified using
458 www.wormbase.org (57). These sequences were codon-optimized for *C. elegans* and
459 cloned in pET-21a(+) cloning vector via XhoI/XhoI strategy by GenScript. The scramble
460 control sequence and plasmid were generated using the same cloning strategy by
461 GenScript. Plasmids arrived lyophilized and were re-suspended in nuclease-free H_2O to
462 a concentration of 100ng/μl and stored at -20 °C. Each expression clone was transformed
463 into competent iOP50 cells using methods previously described(91). Briefly, iOP50 stocks

464 were streaked out onto LB plates containing 50 μg/mL tetracycline and grown at 37 °C
465 overnight. Then, single colonies of iOP50 were isolated and used to inoculate 2.0 mL LB
466 containing 50 μg/ml tetracycline and placed in a 37 °C shaker overnight. 0.5 mL of each
467 culture was used to inoculate 3.0 mL of LB without antibiotics and grown for 2 hours in a
468 37 °C shaker. Each culture was then aliquoted in 0.75 mL increments into four 1.5 mL
469 tubes and cooled for 10 minutes on ice. Next, the cells were harvested by centrifugation
470 at 6,000 rpm for 5 minutes at 4 °C. The resulting supernatant was discarded, and cells
471 were placed back on ice and re-suspended in 1.0 mL 100 mM ice-cold $CaCl_2$ solution.
472 Cells were kept on ice for 20 minutes and then harvested by centrifugation as in the
473 previous step. After discarding the supernatant, cells were re-suspended in 150μl of ice-
474 cold $CaCl_2$ solution and placed on ice to be immediately used for transformation.

475 Competent cells were transformed using the New England Biolabs protocol
476 (C2987H/C2987I). Single colonies of transformed cells were isolated and cultured in 3.0
477 mL of LB containing 50 μg/mL tetracycline and 50 μg/mL carbenicillin overnight in a 37
478 °C shaker. Cultures were frozen down as glycerol stocks and stored at -80 °C. Successful
479 transformation was verified by isolating plasmids from cultures using a Zyppy Plasmid
480 Miniprep Kit and sending samples for whole-plasmid sequencing (Plasmidsaurus).

481 Peptide plate preparation

482 LB containing 50 μg/mL tetracycline and 50 μg/mL carbenicillin was inoculated with iOP50
483 encoding either the peptide sequence of interest or scramble peptide sequence and
484 cultured for 18-20 hours in a 37 °C shaker. 100 mm NGM plates containing 50 μg/mL
485 tetracycline, 50 μg/mL carbenicillin, and 1.0 mL/L isopropyl-β-D-thiogalactoside (IPTG)

486 were plated with 1.0 mL of corresponding culture. Seeded plates were left to dry at least
487 24 hours at room temperature and never kept longer than 72 hours before use.
488 Approximately one hour before transferring worms to peptide or scramble control plates,
489 200 µL of 0.1 M IPTG was added to each plate and left to dry.

490 Peptide feeding

491 We adapted a previously published peptide feeding-based approach (53). Worms were
492 maintained on NGM agar plates seeded with OP50 *E. coli* and maintained at 20 °C until
493 the start of experiments. All animals were transferred to a conical tube and washed three
494 times with M9 buffer solution before being transferred to NGM plates containing 50 μg/mL
495 Tetracycline, 50 μg/mL Carbenicillin, and 1.0 mM IPTG that were seeded with 1.0 mL of
496 iOP50 expressing either the scramble peptide or the peptide of interest. Animals were
497 kept on the scramble or peptide-expressing lawns for at least 48 hours of exposure time
498 at 20 °C before performing assays. Exact peptide feeding timeline parameters are
499 expounded in the results section.

500 RNAi treatment

501 Worms were maintained on NGM agar plates seeded with OP50 *E. coli* at 20 °C until the
502 start of experiments. At the L4 stage, animals were transferred to a conical tube and
503 washed three times with M9 buffer solution before being transferred to NGM plates
504 containing 50 μg/mL Carbenicillin and 1.0 mM IPTG that were seeded with 1.0 mL of
505 HT115 bacteria expressing either RNAi against the gene of interest or the vector control

506 RNAi. Animals were kept on the RNAi lawns for 48 hours of exposure time at 20 °C before
507 performing assays at Day 2 of adulthood.

508 Naïve chemotaxis assay

509 Chemotaxis assays were performed using a protocol based on previously published
510 assays(92). Briefly, assays were performed on unseeded 100mm NGM plates. On the
511 back of each plate, two marks were made on opposite sides of the plate, approximately
512 5mm from the edge. 1μL of sodium azide (Thermo Fisher) was placed on both spots and
513 allowed to dry before adding 1μL of odorant (Sigma Aldrich) diluted in ethanol on one
514 mark and 1μL ethanol on the other. Using M9 buffer, worms were washed off their plates
515 and subsequently washed three times to eliminate any leftover bacteria that could impact
516 baseline behavior. Then, worms were placed near the bottom center of the plate,
517 equidistant between the two marks, and allowed to chemotax for an hour. Chemotaxis
518 indices were calculated as follows:

519 Chemotaxis Index = (# of worms butanone - # of worms ethanol) / (total # of worms)

520 For naïve chemotaxis assays performed to assess baseline chemosensory function, we
521 tested the naïve preference to a highly appetitive concentration of butanone (0.1%) as
522 previously reported (92).

523 Positive associative butanone learning and memory assay

524 Worms were trained and tested for learning, short- and intermediate-term memory
525 changes as previously described (50). Briefly, synchronized adult worms were washed
526 off plates with M9 buffer and allowed to settle by gravity, followed by two subsequent

527 washes with M9 buffer to remove leftover bacteria that could alter baseline behavior.
528 Next, the worms were food-deprived for one hour in M9 buffer before exposure to 1 CS-
529 US pairing, where food-deprived worms were transferred to 100mm NGM conditioning
530 plates seeded with OP50 *E. coli* bacteria (or iOP50 bacteria containing a peptide or
531 scramble control plasmid for peptide feeding experiments) and had 16µL of 10%
532 butanone (Sigma Aldrich) diluted in ethanol streaked on the lid in a '#' shape for one hour.
533 After conditioning, the trained population of worms were tested for chemotaxis to 10%
534 butanone and to an ethanol control using standard, previously described chemotaxis
535 conditions(92). Different stages of memory were tested by measuring chemotaxis indices
536 of separate populations of worms at timepoints including 0 min. (learning), 30 min.
537 (STAM), 60 min. (ITAM) and 120 min. (forgetting) after training. For timepoints after
538 learning behavior, worms were transferred to hold plates seeded with OP50 *E. coli* or
539 iOP50 bacteria for peptide feeding experiments as stated above.

540 Chemotaxis indices for each timepoint were calculated as detailed in "Naïve chemotaxis
541 assays" section.

542 Performance index is the change in the chemotaxis index after training relative to the
543 naïve (untrained) chemotaxis index:

544 Performance index = Chemotaxis $\text{index}_{\text{trained}}$—Chemotaxis $\text{index}_{\text{untrained}}$

545 % Maximum Performance Indices are performance indices represented as a percentage
546 of the maximum value that can be performed relative to the naïve chemotaxis
547 index(31,36). This % can be more informative for visualizing performance indices when
548 naïve chemotaxis behavior is high, as in *daf-2(e1370)* animals. This is calculated for each

549 timepoint by dividing the performance index of a timepoint by the average of the untrained
550 chemotaxis indices of the same behavioral replicate subtracted from 1:

551 % Maximum Performance Index = Performance $index_{timepoint}$/(1 - Chemotaxis $index_{untrained}$)

552 Butanone enhancement assay

553 This assay was adapted from previously described methods (63). Unlike the positive
554 butanone associative memory assays, butanone enhancement assays skip the 1-hour
555 food-deprivation step prior to the conditioning step. All other methods are identical to
556 those listed in the positive butanone associative memory assay section.

557 Negative associative learning and memory assay

558 Worms were tested for learning and memory changes in response to aversive diacetyl
559 training, adapted from previously published methods (68). Similar to positive associative
560 assays, synchronized Day 1 adult worms were washed off plates with M9 buffer and then
561 allowed to settle by gravity and washed twice more with M9 buffer. After washing, the
562 worms were conditioned for one hour by food-deprivation on 100mm NGM plates with no
563 bacteria and 16uL of 100% diacetyl (Sigma Aldrich) streaked on the lid in a '#' shape. The
564 trained population of worms were then tested for chemotaxis to 1% diacetyl and to an
565 ethanol control using standard, previously described chemotaxis conditions (92).
566 Learning and memory performance indices were calculated for each timepoint as
567 previously stated in the positive butanone associative assay section.

568 Lifespan assay

569 Lifespan assays were performed on *ins-17(tm790)* animals and wild-type animals that
570 were bleached onto NGM plates seeded with OP50 *E. coli* and maintained at 20 °C; at
571 the L4 larval stage, worms were picked for survival analysis and transferred every other
572 day to freshly seeded plates. Similarly, lifespan assays with peptide feeding
573 administration were performed on wild-type animals that were bleached onto NGM plates
574 seeded with OP50 *E. coli* and maintained at 20 °C. Then, at the L4 larval stage, worms
575 were picked for survival analysis and transferred every other day to NGM plates
576 containing 50 µg/mL tetracycline, 50 µg/mL carbenicillin, and 1.0 mL/L IPTG that were
577 seeded with either INS-17 iOP50 or scramble iOP50 *E. coli*. Lifespans began (t = 0) at
578 Day 1 of adulthood and had an n = ~120 worms per strain/trial for a total of three biological
579 replicates per assay.

580 Food-deprivation behavioral experiments

581 For food-deprivation experiments, well-fed, synchronized adult worms were washed off
582 plates using M9 buffer into a 15mL conical and washed two more times to remove bacteria
583 that could alter baseline behavior. Next, worms were either 1) food-deprived for one hour
584 on a 100mm NGM plate without food or 2) non-food deprived for one hour by being
585 transferred to a 100mm plate seeded with a bacterial lawn (iOP50 bacteria for peptide
586 feeding experiments). Worms were then immediately exposed to the conditioning step (1
587 CS-US pairing) and stages of learning and memory were tested as stated in the positive
588 associative butanone learning and memory assays section.

589 RNA isolation, cDNA synthesis and qRT-PCR

590 For qRT-PCR food-deprivation experiments, well-fed, synchronized adult worms were
591 washed off plates using M9 buffer into a 15mL conical and washed two more times to
592 remove bacteria that could alter baseline behavior. Next, worms were either 1) food-
593 deprived for one hour or two hours after being transferred to a 100mm plate with no
594 bacterial lawn or 2) non-food deprived for one hour or two hours after being transferred
595 to a 100mm plate seeded with a bacterial lawn.

596 After feeding or food deprivation, worms were crushed in liquid nitrogen using a mortar
597 and pestle and added to Trizol (Thermo Fisher Scientific). RNA was isolated per
598 manufacturer's instructions, followed by DNase treatment (Qiagen). cDNA was
599 synthesized with an oligo dT primer and Superscript III reverse transcriptase enzyme
600 (Thermo Fisher Scientific). cDNA was mixed with buffers, primers, SYBR green, and hot
601 start Taq polymerase in a master mix prepared by a manufacturer (Thermo Fisher
602 Scientific). PCR reactions were run using a Quant Studio 7 Pro Dx Real-Time PCR
603 System (Thermo Fisher Scientific), followed by a dissociation reaction to determine
604 specificity of the amplified product. Gene expression was quantified using the ΔΔCt
605 method using *pmp-3* as a reference gene. Primer sets were as follows:
606 *ins-17* For: 5'- GGACACTATCCGACCACCAC -3':

607 *ins-17* Rev: 5'- TTCACATCCCGTCTCACAGC -3':

608 *pmp-3* For: 5'- AGTTCCGGTTGGATTGGTCC -3'

609 *pmp-3* Rev: 5'- CCAGCACGATAGAAGGCGAT-3'

610 **Statistical analysis and software**

611 All statistics (excluding survival analysis) were calculated with GraphPad Prism Software.
612 All statistical data are reported in the main text, figures, and tables. Significance threshold
613 of $p < 0.05$ was used. The symbols *, **, ***, and **** refer to $p < 0.05$, 0.01, 0.001, and
614 0.0001. The symbols #, ##, ###, and #### refer to $p < 0.05$, 0.01, 0.001, and 0.0001. For
615 comparing performance indices between two behavior conditions (e.g. *vector control*
616 vs *ins-17 RNAi*), we used a Mann-Whitney test comparing ranks, as it does not assume
617 normality. For comparing performance indices between three or more groups (e.g. wild-
618 type vs multiple insulin receptor antagonist mutants), we performed one-way analysis of
619 variances followed by Bonferroni post hoc tests for multiple comparisons. Two-way
620 ANOVAs were used for evaluating effects between genotype and timepoint (T0, T30, T60,
621 T120) on performance indices with a significant interaction between factors ($p<0.0001$)
622 that prompted Bonferroni post-hoc analyses to determine differences between individual
623 groups. Sample size n represents the number of chemotaxis assays performed for
624 behavioral experiments, with each assay containing approximately 50–150 worms. All
625 experiments were performed on different days with distinct populations to confirm
626 reproducibility. For qPCR analysis, unpaired t-tests with Welch's corrections were
627 performed to determine significance between conditions. Survival analysis statistics were
628 generated using the log-rank (Mantel-Cox) method to test the null hypothesis in Kaplan-
629 Meier survival analysis and evaluated using OASIS survival analysis software (93).

630 # Funding

631 RNA was supported by a Glenn Foundation for Medical Research and AFAR Grant for
632 Junior Faculty, the Whitehall Foundation, and an NIH Director's New Innovator Award

(DP2NS132372). EWP is supported by a NIGMS NRSA, EJL is funded by a NIA NRSA. Some strains were provided by the *C. elegans* Genetics Center (CGC), which is funded by the NIH Office of Research Infrastructure Programs (P40 OD010440).

Acknowledgements

We thank the Bargmann lab for generously sharing the *ist-1(ok2706)* strain, and the Caenorhabditis Genetics Center for most other strains used in this publication. We also thank Ben Jussila and In Vivo Biosystems for strains and helpful discussion. Additionally, we especially thank Drs. Buck Samuel and Shinya Yamamoto at Baylor College of Medicine for helpful discussion and advice at various stages of the project. Finally, we thank Arey lab members Katie L. Brandel-Ankrapp and Ty M. Gadberry for feedback on the manuscript.

References:

1. Cooper GM. Pathways of Intracellular Signal Transduction. The Cell: A Molecular Approach [Internet]. 2nd ed. Sinauer Associates; 2000 [cited 2025 Sep 29]. Available from: https://www.ncbi.nlm.nih.gov/books/NBK9870/

2. Li Y, Li S, Wu H. Ubiquitination-Proteasome System (UPS) and Autophagy Two Main Protein Degradation Machineries in Response to Cell Stress. Cells. 2022 Mar 1;11(5).

3. Buscà R, Pouysségur J, Lenormand P. ERK1 and ERK2 map kinases: specific roles or functional redundancy? Front Cell Dev Biol. 2016 Jun 8;4:53.

4. Lefkimmiatis K, Zaccolo M. cAMP signaling in subcellular compartments. Pharmacol Ther. 2014 Sep;143(3):295–304.

657 5. Ullrich A, Bell JR, Chen EY, Herrera R, Petruzzelli LM, Dull TJ, et al. Human
658 insulin receptor and its relationship to the tyrosine kinase family of oncogenes.
659 Nature. 1985;313(6005):756–61.

660 6. Ullrich A, Gray A, Tam AW, Yang-Feng T, Tsubokawa M, Collins C, et al.
661 Insulin-like growth factor I receptor primary structure: comparison with insulin
662 receptor suggests structural determinants that define functional specificity. EMBO
663 J. 1986 Oct;5(10):2503–12.

664 7. White MF. The IRS-signalling system: a network of docking proteins that
665 mediate insulin action. Mol Cell Biochem. 1998 May;182(1–2):3–11.

666 8. Taniguchi CM, Emanuelli B, Kahn CR. Critical nodes in signalling pathways:
667 insights into insulin action. Nat Rev Mol Cell Biol. 2006 Feb;7(2):85–96.

668 9. Piñero González J, Carrillo Farnés O, Vasconcelos ATR, González Pérez A.
669 Conservation of key members in the course of the evolution of the insulin
670 signaling pathway. BioSystems. 2009 Jan;95(1):7–16.

671 10. Kaletsky R, Murphy CT. The role of insulin/IGF-like signaling in C. elegans
672 longevity and aging. Dis Model Mech. 2010 Aug 1;3(7–8):415–9.

673 11. Finch CE, Ruvkun G. The genetics of aging. Annu Rev Genomics Hum Genet.
674 2001;2:435–62.

675 12. Murphy CT, Hu PJ. Insulin/insulin-like growth factor signaling in C. elegans.
676 WormBook. 2013 Dec 26;1–43.

677 13. Semaniuk U, Piskovatska V, Strilbytska O, Strutynska T, Burdyliuk N, Vaiserman
678 A, et al. *Drosophila* insulin-like peptides: from expression to functions – a review.
679 Entomol Exp Appl. 2021 Feb;169(2):195–208.

680 14. Biglou SG, Bendena WG, Chin-Sang I. An overview of the insulin signaling
681 pathway in model organisms Drosophila melanogaster and Caenorhabditis
682 elegans. Peptides. 2021 Nov;145:170640.

683 15. Suzawa M, Bland ML. Insulin signaling in development. Development. 2023 Oct
684 15;150(20).

685 16. Barbieri M, Bonafè M, Franceschi C, Paolisso G. Insulin/IGF-I-signaling
686 pathway: an evolutionarily conserved mechanism of longevity from yeast to
687 humans. Am J Physiol Endocrinol Metab. 2003 Nov;285(5):E1064-71.

688 17. Lau HE, Chalasani SH. Divergent and convergent roles for insulin-like peptides
689 in the worm, fly and mammalian nervous systems. Invert Neurosci. 2014
690 Sep;14(2):71–8.

691 18. Hales KG, Korey CA, Larracuente AM, Roberts DM. Genetics on the fly: A
692 primer on the drosophila model system. Genetics. 2015 Nov;201(3):815–42.

693 19. Boulin T, Hobert O. From genes to function: the C. elegans genetic toolbox.
694 Wiley Interdiscip Rev Dev Biol. 2012 Feb;1(1):114–37.

695 20. Simone BW, Martínez-Gálvez G, WareJoncas Z, Ekker SC. Fishing for
696 understanding: Unlocking the zebrafish gene editor's toolbox. Methods. 2018 Nov
697 1;150:3–10.

698 21. Kenyon C, Chang J, Gensch E, Rudner A, Tabtiang R. A C. elegans mutant that
699 lives twice as long as wild type. Nature. 1993 Dec 2;366(6454):461–4.

700 22. Friedman DB, Johnson TE. A mutation in the age-1 gene in Caenorhabditis
701 elegans lengthens life and reduces hermaphrodite fertility. Genetics. 1988
702 Jan;118(1):75–86.

703 23. Hsu A-L, Murphy CT, Kenyon C. Regulation of aging and age-related disease by
704 DAF-16 and heat-shock factor. Science. 2003 May 16;300(5622):1142–5.

705 24. An JH, Blackwell TK. SKN-1 links C. elegans mesendodermal specification to a
706 conserved oxidative stress response. Genes Dev. 2003 Aug 1;17(15):1882–93.

707 25. Morris JZ, Tissenbaum HA, Ruvkun G. A phosphatidylinositol-3-OH kinase
708 family member regulating longevity and diapause in Caenorhabditis elegans.
709 Nature. 1996 Aug 8;382(6591):536–9.

710 26. Kimura KD, Tissenbaum HA, Liu Y, Ruvkun G. daf-2, an insulin receptor-like
711 gene that regulates longevity and diapause in Caenorhabditis elegans. Science.
712 1997 Aug 15;277(5328):942–6.

713 27. Lin K, Dorman JB, Rodan A, Kenyon C. daf-16: An HNF-3/forkhead family
714 member that can function to double the life-span of Caenorhabditis elegans.
715 Science. 1997 Nov 14;278(5341):1319–22.

716 28. Ogg S, Paradis S, Gottlieb S, Patterson GI, Lee L, Tissenbaum HA, et al. The
717 Fork head transcription factor DAF-16 transduces insulin-like metabolic and
718 longevity signals in C. elegans. Nature. 1997 Oct 30;389(6654):994–9.

719 29. Luo S, Kleemann GA, Ashraf JM, Shaw WM, Murphy CT. TGF-β and insulin
720 signaling regulate reproductive aging via oocyte and germline quality
721 maintenance. Cell. 2010 Oct 15;143(2):299–312.

722 30. Mulcahy B, Holden-Dye L, O'Connor V. Pharmacological assays reveal age-
723 related changes in synaptic transmission at the Caenorhabditis elegans

724 neuromuscular junction that are modified by reduced insulin signalling. J Exp
725 Biol. 2013 Feb 1;216(Pt 3):492–501.

726 31. Kauffman AL, Ashraf JM, Corces-Zimmerman MR, Landis JN, Murphy CT.
727 Insulin signaling and dietary restriction differentially influence the decline of
728 learning and memory with age. PLoS Biol. 2010 May 18;8(5):e1000372.

729 32. Riddle DL, Swanson MM, Albert PS. Interacting genes in nematode dauer larva
730 formation. Nature. 1981 Apr 23;290(5808):668–71.

731 33. Gems D, Sutton AJ, Sundermeyer ML, Albert PS, King KV, Edgley ML, et al.
732 Two pleiotropic classes of daf-2 mutation affect larval arrest, adult behavior,
733 reproduction and longevity in Caenorhabditis elegans. Genetics. 1998
734 Sep;150(1):129–55.

735 34. Ange JS, Weng Y, Stevenson ME, Kaletsky R, Moore RS, Zhou S, et al. Adult
736 Single-nucleus Neuronal Transcriptomes of Insulin Signaling Mutants Reveal
737 Regulators of Behavior and Learning. BioRxiv. 2024 Feb 7;

738 35. Templeman NM, Luo S, Kaletsky R, Shi C, Ashraf J, Keyes W, et al. Insulin
739 Signaling Regulates Oocyte Quality Maintenance with Age via Cathepsin B
740 Activity. Curr Biol. 2018 Mar 5;28(5):753-760.e4.

741 36. Weng Y, Zhou S, Morillo K, Kaletsky R, Lin S, Murphy CT. The neuron-specific
742 IIS/FOXO transcriptome in aged animals reveals regulatory mechanisms of
743 cognitive aging. eLife. 2024 Jun 26;13.

744 37. Zhou S, Novak KE, Kaletsky R, Weng Y, Ange JS, Stevenson ME, et al. Body-
745 to-brain insulin and Notch signaling regulates memory through neuronal CREB
746 activity. Nat Aging. 2025 Jul;5(7):1232–48.

747 38. Hughes SE, Evason K, Xiong C, Kornfeld K. Genetic and pharmacological
748 factors that influence reproductive aging in nematodes. PLoS Genet. 2007 Feb
749 16;3(2):e25.

750 39. Lin K, Hsin H, Libina N, Kenyon C. Regulation of the Caenorhabditis elegans
751 longevity protein DAF-16 by insulin/IGF-1 and germline signaling. Nat Genet.
752 2001 Jun;28(2):139–45.

753 40. Hahm J-H, Kim S, DiLoreto R, Shi C, Lee S-JV, Murphy CT, et al. C. elegans
754 maximum velocity correlates with healthspan and is maintained in worms with an
755 insulin receptor mutation. Nat Commun. 2015 Nov 20;6:8919.

756 41. Bansal A, Zhu LJ, Yen K, Tissenbaum HA. Uncoupling lifespan and healthspan
757 in Caenorhabditis elegans longevity mutants. Proc Natl Acad Sci USA. 2015 Jan
758 20;112(3):E277-86.

759 42. Roy C, Molin L, Alcolei A, Solyga M, Bonneau B, Vachon C, et al. DAF-2/insulin
760 IGF-1 receptor regulates motility during aging by integrating opposite signaling
761 from muscle and neuronal tissues. Aging Cell. 2022 Aug;21(8):e13660.

762 43. Duret L, Guex N, Peitsch MC, Bairoch A. New insulin-like proteins with atypical
763 disulfide bond pattern characterized in Caenorhabditis elegans by comparative
764 sequence analysis and homology modeling. Genome Res. 1998 Apr;8(4):348–
765 53.

766 44. Kawano T, Ito Y, Ishiguro M, Takuwa K, Nakajima T, Kimura Y. Molecular
767 cloning and characterization of a new insulin/IGF-like peptide of the nematode
768 Caenorhabditis elegans. Biochem Biophys Res Commun. 2000 Jul 5;273(2):431–
769 6.

770 45. Pierce SB, Costa M, Wisotzkey R, Devadhar S, Homburger SA, Buchman AR, et
771 al. Regulation of DAF-2 receptor signaling by human insulin and ins-1, a member
772 of the unusually large and diverse C. elegans insulin gene family. Genes Dev.
773 2001 Mar 15;15(6):672–86.

774 46. Li W, Kennedy SG, Ruvkun G. daf-28 encodes a C. elegans insulin superfamily
775 member that is regulated by environmental cues and acts in the DAF-2 signaling
776 pathway. Genes Dev. 2003 Apr 1;17(7):844–58.

777 47. Zheng S, Chiu H, Boudreau J, Papanicolaou T, Bendena W, Chin-Sang I. A
778 functional study of all 40 Caenorhabditis elegans insulin-like peptides. J Biol
779 Chem. 2018 Oct 26;293(43):16912–22.

780 48. Ritter AD, Shen Y, Fuxman Bass J, Jeyaraj S, Deplancke B, Mukhopadhyay A,
781 et al. Complex expression dynamics and robustness in C. elegans insulin
782 networks. Genome Res. 2013 Jun;23(6):954–65.

783 49. Matsunaga Y, Nakajima K, Gengyo-Ando K, Mitani S, Iwasaki T, Kawano T. A
784 Caenorhabditis elegans insulin-like peptide, INS-17: its physiological function and
785 expression pattern. Biosci Biotechnol Biochem. 2012 Nov 7;76(11):2168–72.

786 50. Kauffman A, Parsons L, Stein G, Wills A, Kaletsky R, Murphy C. C. elegans
787 positive butanone learning, short-term, and long-term associative memory
788 assays. J Vis Exp. 2011 Mar 11;(49).

789 51. Chen Y, Baugh LR. Ins-4 and daf-28 function redundantly to regulate C. elegans
790 L1 arrest. Dev Biol. 2014 Oct 15;394(2):314–26.

791 52. Zhu R, Chin-Sang ID. C. elegans insulin-like peptides. Mol Cell Endocrinol. 2024
792 May 1;585:112173.

793 53. DiLoreto EM, Shastry S, Leptich EJ, Reilly DK, Arey RN, Srinivasan J.
794 Harnessing Microbial Tools: Escherichia coli as a Vehicle for Neuropeptide
795 Functional Analysis in Caenorhabditis elegans. Genetics. 2025 Aug 6;

796 54. Kamath RS, Ahringer J. Genome-wide RNAi screening in Caenorhabditis
797 elegans. Methods. 2003 Aug;30(4):313–21.

798 55. Yang Y, Arnold ML, Lange CM, Sun L-H, Broussalian M, Doroodian S, et al.
799 Autophagy protein ATG-16.2 and its WD40 domain mediate the beneficial effects
800 of inhibiting early-acting autophagy genes in C. elegans neurons. Nat Aging.
801 2024 Feb;4(2):198–212.

802 56. Murphy CT, McCarroll SA, Bargmann CI, Fraser A, Kamath RS, Ahringer J, et al.
803 Genes that act downstream of DAF-16 to influence the lifespan of Caenorhabditis
804 elegans. Nature. 2003 Jul 17;424(6946):277–83.

805 57. Sternberg PW, Van Auken K, Wang Q, Wright A, Yook K, Zarowiecki M, et al.
806 WormBase 2024: status and transitioning to Alliance infrastructure. Genetics.
807 2024 May 7;227(1).

808 58. Taylor SR, Santpere G, Weinreb A, Barrett A, Reilly MB, Xu C, et al. Molecular
809 topography of an entire nervous system. Cell. 2021 Aug 5;184(16):4329-
810 4347.e23.

811 59. Mueller MM, Castells-Roca L, Babu V, Ermolaeva MA, Müller R-U, Frommolt P,
812 et al. DAF-16/FOXO and EGL-27/GATA promote developmental growth in
813 response to persistent somatic DNA damage. Nat Cell Biol. 2014
814 Dec;16(12):1168–79.

815 60. Hibshman JD, Doan AE, Moore BT, Kaplan RE, Hung A, Webster AK, et al. daf-
816 16/FoxO promotes gluconeogenesis and trehalose synthesis during starvation to
817 support survival. eLife. 2017 Oct 24;6.

818 61. St Ange J, Weng Y, Kaletsky R, Stevenson ME, Moore RS, Zhou S, et al. Adult
819 single-nucleus neuronal transcriptomes of insulin signaling mutants reveal
820 regulators of behavior and learning. Cell Genomics. 2024 Dec 11;4(12):100720.

821 62. Ogawa T, Isik M, Wu Z, Kurmi K, Meng J, Cho S, et al. Nutrient control of growth
822 and metabolism through mTORC1 regulation of mRNA splicing. Mol Cell. 2024
823 Dec 5;84(23):4558-4575.e8.

824 63. Torayama I, Ishihara T, Katsura I. Caenorhabditis elegans integrates the signals
825 of butanone and food to enhance chemotaxis to butanone. J Neurosci. 2007 Jan
826 24;27(4):741–50.

827 64. Baugh LR, Hu PJ. Starvation responses throughout the caenorhabditiselegans
828 life cycle. Genetics. 2020 Dec;216(4):837–78.

829 65. Ben Arous J, Laffont S, Chatenay D. Molecular and sensory basis of a food
830 related two-state behavior in C. elegans. PLoS ONE. 2009 Oct 23;4(10):e7584.

831 66. Kimura KD, Riddle DL, Ruvkun G. The C. elegans DAF-2 insulin-like receptor is
832 abundantly expressed in the nervous system and regulated by nutritional status.
833 Cold Spring Harb Symp Quant Biol. 2011 Nov 28;76:113–20.

834 67. Venz R, Pekec T, Katic I, Ciosk R, Ewald CY. End-of-life targeted degradation of
835 DAF-2 insulin/IGF-1 receptor promotes longevity free from growth-related
836 pathologies. eLife. 2021 Sep 10;10.

837 68. Stetak A, Hörndli F, Maricq AV, van den Heuvel S, Hajnal A. Neuron-specific
838 regulation of associative learning and memory by MAGI-1 in C. elegans. PLoS
839 ONE. 2009 Jun 24;4(6):e6019.

840 69. Fadda M, De Fruyt N, Borghgraef C, Watteyne J, Peymen K, Vandewyer E, et
841 al. NPY/NPF-Related Neuropeptide FLP-34 Signals from Serotonergic Neurons
842 to Modulate Aversive Olfactory Learning in Caenorhabditis elegans. J Neurosci.
843 2020 Jul 29;40(31):6018–34.

844 70. Choi JI, Lee HK, Kim HS, Park SY, Lee TY, Yoon K-H, et al. Odor-dependent
845 temporal dynamics in Caenorhabitis elegans adaptation and aversive learning
846 behavior. PeerJ. 2018 Jun 12;6:e4956.

847 71. Amano H, Maruyama IN. Aversive olfactory learning and associative long-term
848 memory in Caenorhabditis elegans. Learn Mem. 2011 Oct;18(10):654–65.

849 72. Chen Z, Hendricks M, Cornils A, Maier W, Alcedo J, Zhang Y. Two insulin-like
850 peptides antagonistically regulate aversive olfactory learning in C. elegans.
851 Neuron. 2013 Feb 6;77(3):572–85.

852 73. Ha H, Hendricks M, Shen Y, Gabel CV, Fang-Yen C, Qin Y, et al. Functional
853 organization of a neural network for aversive olfactory learning in Caenorhabditis
854 elegans. Neuron. 2010 Dec 22;68(6):1173–86.

855 74. O'Halloran DM, Altshuler-Keylin S, Lee JI, L'Etoile ND. Regulators of AWC-
856 mediated olfactory plasticity in Caenorhabditis elegans. PLoS Genet. 2009 Dec
857 11;5(12):e1000761.

858 75. Chalasani SH, Kato S, Albrecht DR, Nakagawa T, Abbott LF, Bargmann CI.
859 Neuropeptide feedback modifies odor-evoked dynamics in Caenorhabditis
860 elegans olfactory neurons. Nat Neurosci. 2010 May;13(5):615–21.

861 76. Mendler M, Riedinger C, Schlotterer A, Volk N, Fleming T, Herzig S, et al.
862 Reduction in ins-7 gene expression in non-neuronal cells of high glucose
863 exposed Caenorhabditis elegans protects from reactive metabolites, preserves
864 neuronal structure and head motility, and prolongs lifespan. J Diabetes
865 Complicat. 2017 Feb;31(2):304–10.

866 77. Chen J, Scheiner AR, Falsztyn IB, Baugh LR. ist-1/IRS1 affects L1 starvation
867 resistance in daf-16/FoxO- dependent and independent fashion. MicroPubl Biol.
868 2025 Jun 13;2025.

869 78. Wolkow CA, Muñoz MJ, Riddle DL, Ruvkun G. Insulin receptor substrate and
870 p55 orthologous adaptor proteins function in the Caenorhabditis elegans daf-
871 2/insulin-like signaling pathway. J Biol Chem. 2002 Dec 20;277(51):49591–7.

872 79. Cheng D, Lee JS, Brown M, Ebert MS, McGrath PT, Tomioka M, et al.
873 Insulin/IGF signaling regulates presynaptic glutamate release in aversive
874 olfactory learning. Cell Rep. 2022 Nov 22;41(8):111685.

875 80. Matty MA, Lau HE, Haley JA, Singh A, Chakraborty A, Kono K, et al. Intestine-
876 to-neuronal signaling alters risk-taking behaviors in food-deprived Caenorhabditis
877 elegans. PLoS Genet. 2022 May 5;18(5):e1010178.

878 81. Viri V, Arveiler M, Lehnert T, Gijs MAM. An In Vivo Microfluidic Study of Bacterial
879 Load Dynamics and Absorption in the C. elegans Intestine. Micromachines
880 (Basel). 2021 Jul 17;12(7).

881 82. Ghafouri S, McGhee JD. Bacterial residence time in the intestine of
882 Caenorhabditis elegans. Nematol. 2007;9(1):87–91.

883 83. Cassada RC, Russell RL. The dauerlarva, a post-embryonic developmental
884 variant of the nematode Caenorhabditis elegans. Dev Biol. 1975 Oct;46(2):326–
885 42.

886 84. Weinshenker D, Garriga G, Thomas JH. Genetic and pharmacological analysis
887 of neurotransmitters controlling egg laying in C. elegans. J Neurosci. 1995
888 Oct;15(10):6975–85.

889 85. Kuhara A, Mori I. Molecular physiology of the neural circuit for calcineurin-
890 dependent associative learning in Caenorhabditis elegans. J Neurosci. 2006 Sep
891 13;26(37):9355–64.

892 86. Tsalik EL, Hobert O. Functional mapping of neurons that control locomotory
893 behavior in Caenorhabditis elegans. J Neurobiol. 2003 Aug;56(2):178–97.

894 87. Iino Y, Yoshida K. Parallel use of two behavioral mechanisms for chemotaxis in
895 Caenorhabditis elegans. J Neurosci. 2009 Apr 29;29(17):5370–80.

896 88. Li H, Namburi P, Olson JM, Borio M, Lemieux ME, Beyeler A, et al. Neurotensin
897 orchestrates valence assignment in the amygdala. Nature. 2022
898 Aug;608(7923):586–92.

899 89. Kim D-I, Kang SJ, Jhang J, Jo YS, Park S, Ye M, et al. Encoding opposing
900 valences through frequency-dependent transmitter switching in single peptidergic
901 neurons. bioRxiv. 2024 Jan 1;

902 90. Brenner S. The genetics of Caenorhabditis elegans. Genetics. 1974
903 May;77(1):71–94.

904 91. Neve IAA, Sowa JN, Lin C-CJ, Sivaramakrishnan P, Herman C, Ye Y, et al.
905 Escherichia coli Metabolite Profiling Leads to the Development of an RNA
906 Interference Strain for Caenorhabditis elegans. G3 (Bethesda). 2020 Jan
907 7;10(1):189–98.

908 92. Bargmann CI, Hartwieg E, Horvitz HR. Odorant-selective genes and neurons
909 mediate olfaction in C. elegans. Cell. 1993 Aug 13;74(3):515–27.

910 93. Yang J-S, Nam H-J, Seo M, Han SK, Choi Y, Nam HG, et al. OASIS: online
911 application for the survival analysis of lifespan assays performed in aging research.
912 PLoS ONE. 2011 Aug 15;6(8):e23525.

913

914 # Figure legends

915 **Fig. 1. INS-17 is a novel and specific memory-regulating insulin receptor antagonist**

916 **(A)** Partial loss-of-function *daf-2(e1370)* mutants have extended STAM that lasts 6 hours
917 compared to 2 hours for wild-type animals after 1 CS-US food-butanone pairing. % Max
918 Performance reported as *daf-2(e1370)* animals have a higher baseline naïve attraction to
919 neutral (10%) butanone concentration (see **Fig. S1A, B**). Mean ± SEM. n = 15 per
920 genotype. **(B)** Diagram depicting the hypothesis that insulin receptor antagonists may
921 inhibit DAF-2 receptor function to promote learning and memory. **(C)** *ins-17* deletion
922 mutants have impaired learning, STAM, and ITAM compared to wild-type worms. Mean ±
923 SEM. n = 15 per genotype. ***$p < 0.001$, ****$p < 0.001$; ns, not significant ($p > 0.05$). **(D)**

924 Weak insulin antagonist mutants for *ins-15* and *ins-21* and **(E)** strong insulin antagonist
925 mutants for *ins-37* and *ins-39* display no memory impairments; *ins-39* mutants have better
926 ITAM performance compared to wild-type. Mean ± SEM. n = 15 per genotype. ***p <
927 0.001.

928 **Fig. 2. INS-17 and DAF-2 are epistatic and promote memory**

929 **(A)** *daf-2* and *ins-17* share an epistatic relationship. 3hrs post-training (1 CS-US pairing),
930 *daf-2(e1370)* mutants and *daf-2(e1370)*;*ins-17(tm790)* double mutants display memory
931 behavior while *ins-17(tm790)* animals display no memory behavior. Mean ± SEM. n = 15
932 per genotype. ****p < 0.0001. **(B)** Diagram of microbial feeding paradigm. iOP50 bacteria
933 were transformed with a plasmid containing either the peptide sequence of interest or a
934 scramble control sequence and then fed to worms before testing behavioral effects. **(C)**
935 INS-17 peptide feeding rescues *ins-17(tm790)* learning, STAM and ITAM behaviors, while
936 SCR fed mutants display significant S/ITAM impairments compared to SCR fed wild-type
937 animals. Mean ± SEM. n = 15 per feeding treatment. # is significance relative to SCR fed
938 wild-type animal performance. ###p < 0.001, ####p < 0.0001; ns, not significant (p >
939 0.05). **(D)** Wild-type animals fed INS-17 peptides display 3-hour memory behavior after 1
940 CS-US pairing, similar to *daf-2(e1370)* extended STAM performance. Mean ± SEM. n =
941 15 per peptide treatment. ****p < 0.0001. **(E)** Adult-only, neuron-specific RNAi knock-
942 down of *ins-17* leads to learning, STAM, and ITAM impairments compared to vector RNAi
943 treated animals. Mean ± SEM. n = 15 per RNAi treatment. ****p < 0.0001.

944 **Fig. 3. INS-17 regulates cognitive aging phenotypes observed in *daf-2* mutants**

945 **(A)** Day 5 adult *daf-2(e1370)* mutants display better learning and **(B)** memory behavior
946 compared to wild-type worms. Mean ± SEM. n = 10 per genotype. *p < 0.05, *** p < 0.001.
947 **(C)** Timeline of young adult peptide treatment. Wild-type L4 animals are fed SCR or INS-
948 17 iOP50 bacteria until Day 5 of adulthood when S/ITAM behavior is tested. INS-17
949 peptide treated worms have increased learning and **(D)** ITAM performance compared to
950 SCR peptide treated animals. Mean ± SEM. n = 15 per peptide treatment. *p < 0.05. **(E)**
951 Timeline of aged adult peptide treatment. Wild-type Day 3 adult animals are fed SCR or
952 INS-17 iOP50 bacteria until Day 5 of adulthood when S/ITAM behavior is tested. INS-17
953 peptide treated worms have increased learning performance, but not **(F)** ITAM
954 performance, compared to SCR peptide treated animals. Mean ± SEM. n = 15 per peptide
955 treatment. *p < 0.05, ****p < 0.0001. **(G)** Probability of survival analysis demonstrates
956 there is no significant difference in lifespan comparing wild-type animals and *ins-*
957 *17(tm790)* animals. One replicate depicted is representative of three replicates (see **Fig.**
958 **S3F, S3G**). Mean/median ± SEM. n ≥ 100 per replicate. ns, not significant (p > 0.05). **(H)**
959 Probability of survival analysis for wild-type animals treated with SCR peptide compared
960 to wild-type animals fed INS-17 peptide shows no significant difference in average
961 lifespan. One replicate depicted is representative of three replicates (see **Fig. S3H, S3I**).
962 Mean/median ± SEM. n ≥ 100 per replicate. ns, not significant (p > 0.05).

963 **Fig. 4. INS-17 likely engages parallel pathways of DAF-2 receptor signaling**

964 **(A)** *daf-16(mu86)* deletion mutants have impaired learning and memory behavior
965 compared to wild-type animals. Mean ± SEM. n = 15 per genotype. ****p < 0.0001. **(B)**
966 INS-17 peptide treatment rescues *daf-16(mu86)* S/ITAM impairments. Mean ± SEM. n =

967 15 per genotype and peptide treatment. Wild-type animals fed INS-17 performance
968 indices are in **Fig. S4C**. # is significance relative to wild-type. #p < 0.05, ##p < 0.01; ns,
969 not significant (p > 0.05). **(C)** *ist-1(ok2706)* deletion mutants display a slight but not
970 significant learning deficit and impaired S/ITAM behaviors compared to wild-type worms.
971 Mean ± SEM. n = 15 per genotype. *p < 0.05, **p < 0.01; ns, not significant (p > 0.05).
972 **(D)** INS-17 peptide treatment rescues *ist-1(ok2706)* learning and memory impairments.
973 Mean ± SEM. n = 15 per genotype and peptide treatment. # is significance relative to
974 wild-type. #p < 0.05, ##p < 0.01, ###p < 0.001, ****p< 0.0001; ns, not significant (p >
975 0.05). **(E)** *daf-16(mu86)*;*ist-1(ok2706)* animals display significant learning and **(F)**
976 memory impairments that are not rescued by INS-17 peptide feeding, while *daf-16(mu86)*
977 and *ist-1(ok2706)* deficits are rescued by INS-17 peptide administration. Mean ± SEM. n
978 = 15 per genotype and peptide treatment *p < 0.05, **p < 0.01, ***p < 0.001; ns, not
979 significant (p > 0.05).

980 **Fig. 5. INS-17 is regulated by nutrient deprivation to promote advantageous**
981 **behaviors**

982 **(A)** Diagram showing *ins-17* replacement experiment design. *ins-17* and *ins-37* encode γ
983 -ILPs. *ins-17* was removed with CRISPR and replaced with *ins-37* at the *ins-17* locus so
984 *ins-37* would be expressed at endogenous *ins-17* levels. **(B)** Replacing *ins-17* with *ins-*
985 *37* has no significant effect on behavior compared to wild-type animals, while *ins-17*
986 CRISPR KO (*ins-17(knu1320)*) animals have impaired learning and S/ITAM. Mean ±
987 SEM. n = 15 per genotype. # is significance relative to wild-type. ####p < 0.0001; ns, not
988 significant (p > 0.05). **(C)** qRT-PCR of *ins-17* mRNA levels in Day 1 adult wild-type animals
989 show that one hour of food-deprivation (FD) results in increased *ins-17* transcript levels

990 (left). For levels measured after two hours of food-deprivation, please see **Fig. S5B.**
991 Schematic depicting food-deprivation experiment workflow (right): well-fed adult worms
992 are washed three times in M9 buffer solution to remove bacteria and placed on 100mm
993 agar plates either seeded with a bacterial lawn (non-FD) or no lawn (FD) prior to training
994 and behavior testing. Mean ± SEM. n = 5 per genotype. *p < 0.05. **(D)** Wild-type animals
995 display more robust ITAM behavior if a FD step is administered prior to 1 CS-US pairing
996 compared to training alone (non-FD conditions). Mean ± SEM. n = 15 per condition. *p <
997 0.05. **(E)** Food-deprivation prior to training (1 CS-US pairing) does not enhance *daf-*
998 *2(e1370)* ITAM performance. Mean ± SEM. n = 15 per condition. ns, not significant (p >
999 0.05). **(F)** INS-17 peptide treatment in wild-type animals is sufficient to promote robust
1000 ITAM performance in non-FD conditions prior to training compared to non-FD SCR fed
1001 animals. See **Fig. S5I** for food-deprived SCR and INS-17 peptide fed comparisons. Mean
1002 ± SEM. n = 15 per peptide treatment. **p < 0.01. **(G)** *ins-17(tm790)* mutants have
1003 significantly impaired aversive associative learning and STAM performance compared to
1004 wild-type worms. Absolute values of learning and memory performance indices are
1005 reported. Mean ± SEM. n = 15 per genotype. ***p < 0.001, ****p < 0.0001; ns, not
1006 significant (p > 0.05). **(H)** Putative diagram of how INS-17 is upregulated in the nervous
1007 system to signal the valence of positive and aversive environmental conditions to inform
1008 behavioral outputs advantageous for survival.

1009

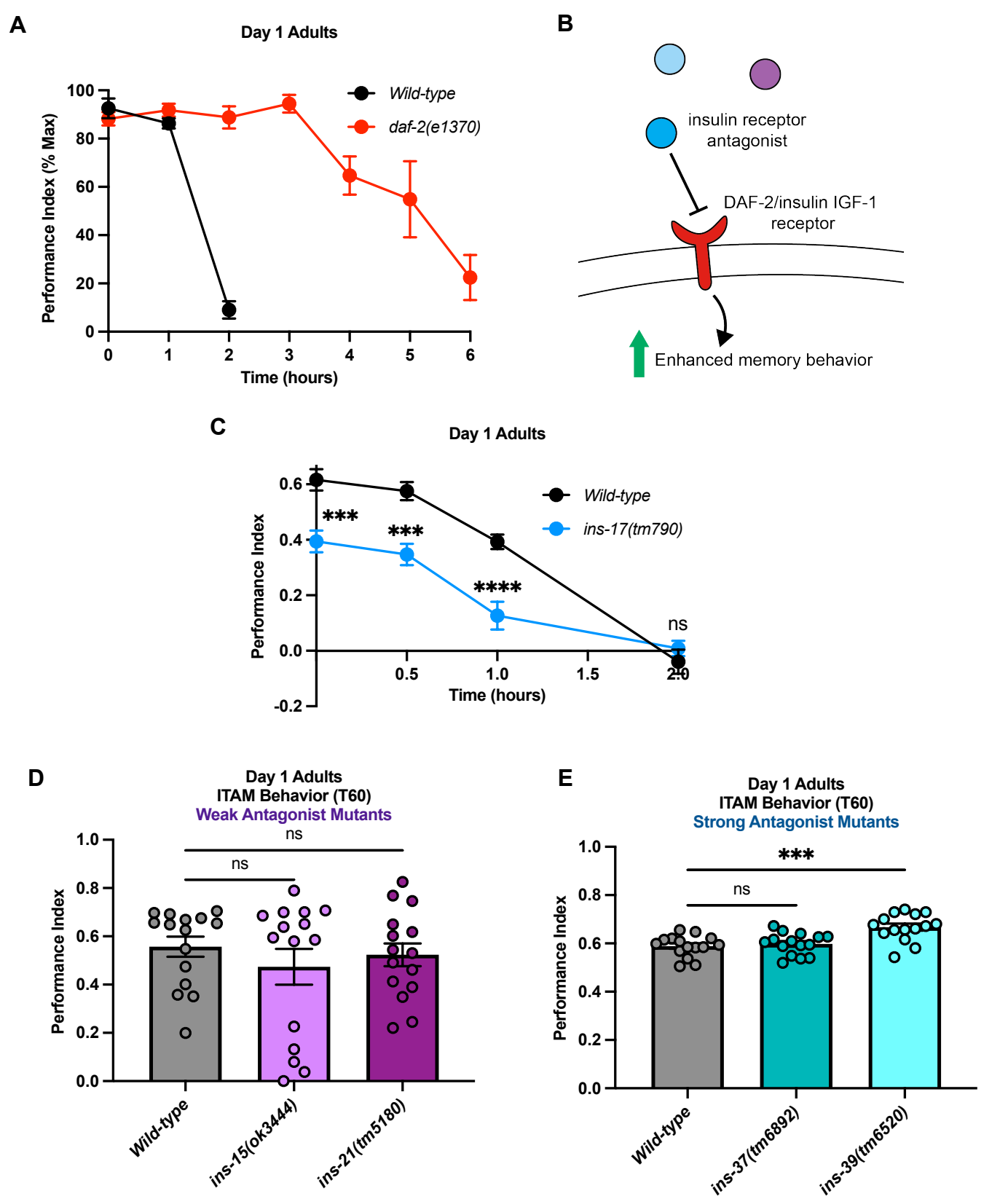
A
Day 1 Adults
Performance Index (% Max)
Time (hours)
Wild-type
daf-2(e1370)
B
insulin receptor antagonist
DAF-2/insulin IGF-1 receptor
Enhanced memory behavior
C
Day 1 Adults
Performance Index
Time (hours)
Wild-type
ins-17(tm790)
***
***
****
ns
D
Day 1 Adults
ITAM Behavior (T60)
Weak Antagonist Mutants
Performance Index
ns
ns
Wild-type
ins-15(ok3444)
ins-21(tm5180)
E
Day 1 Adults
ITAM Behavior (T60)
Strong Antagonist Mutants
Performance Index
***
ns
Wild-type
ins-37(tm6892)
ins-39(tm6520)

Figure 1

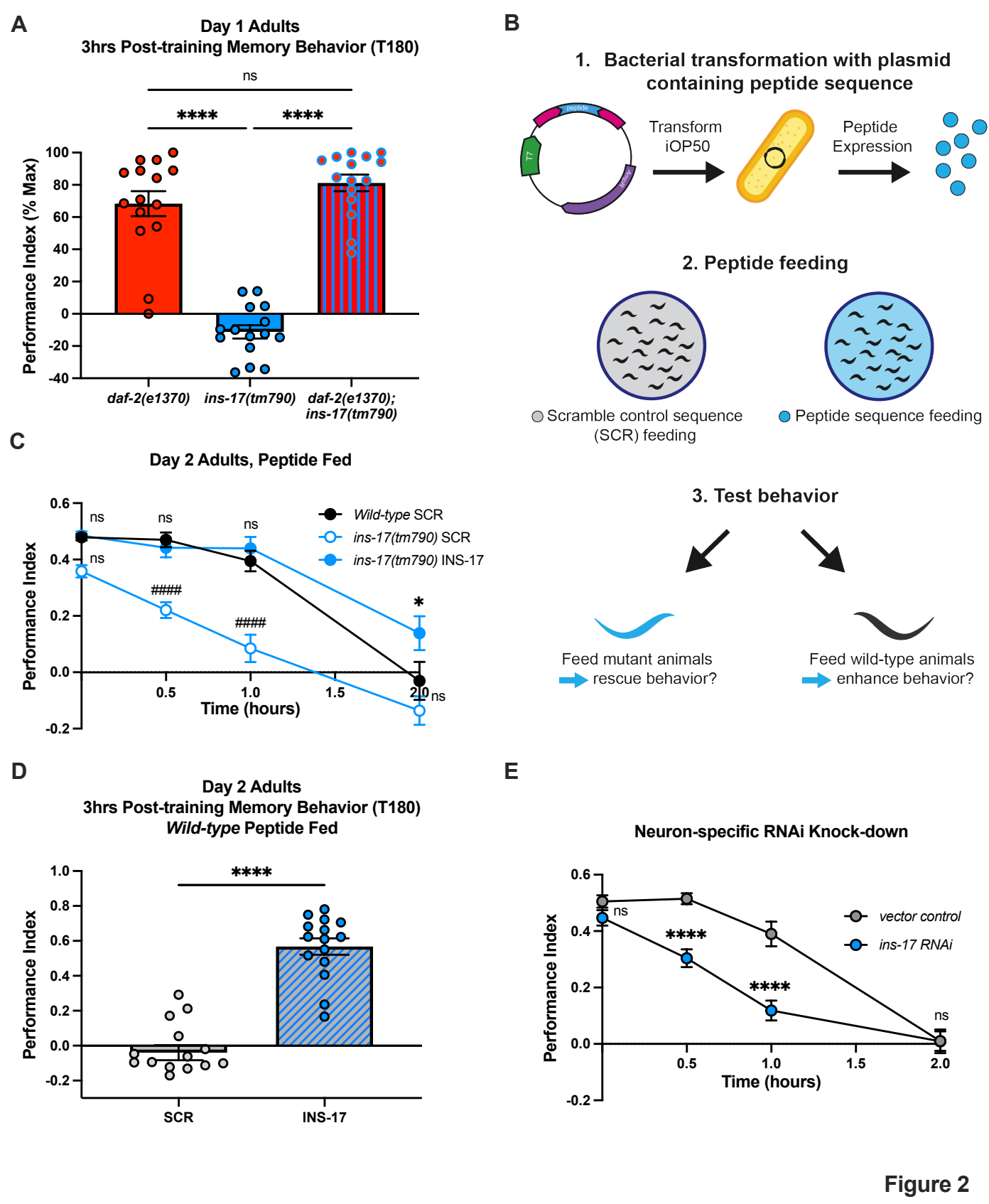
A
Day 1 Adults
3hrs Post-training Memory Behavior (T180)
ns
****
****
Performance Index (% Max)
100
80
60
40
20
0
-20
-40
daf-2(e1370)
ins-17(tm790)
daf-2(e1370); ins-17(tm790)
B
1. Bacterial transformation with plasmid containing peptide sequence
Transform iOP50
Peptide Expression
2. Peptide feeding
Scramble control sequence (SCR) feeding
Peptide sequence feeding
3. Test behavior
Feed mutant animals rescue behavior?
Feed wild-type animals enhance behavior?
C
Day 2 Adults, Peptide Fed
Performance Index
0.6
0.4
0.2
0.0
-0.2
ns
ns
ns
ns
####
####
*
ns
0.5
1.0
1.5
2.0
Time (hours)
Wild-type SCR
ins-17(tm790) SCR
ins-17(tm790) INS-17
D
Day 2 Adults
3hrs Post-training Memory Behavior (T180)
Wild-type Peptide Fed
****
Performance Index
1.0
0.8
0.6
0.4
0.2
0.0
-0.2
SCR
INS-17
E
Neuron-specific RNAi Knock-down
Performance Index
0.6
0.4
0.2
0.0
-0.2
ns
****
****
ns
0.5
1.0
1.5
2.0
Time (hours)
vector control
ins-17 RNAi

Figure 2

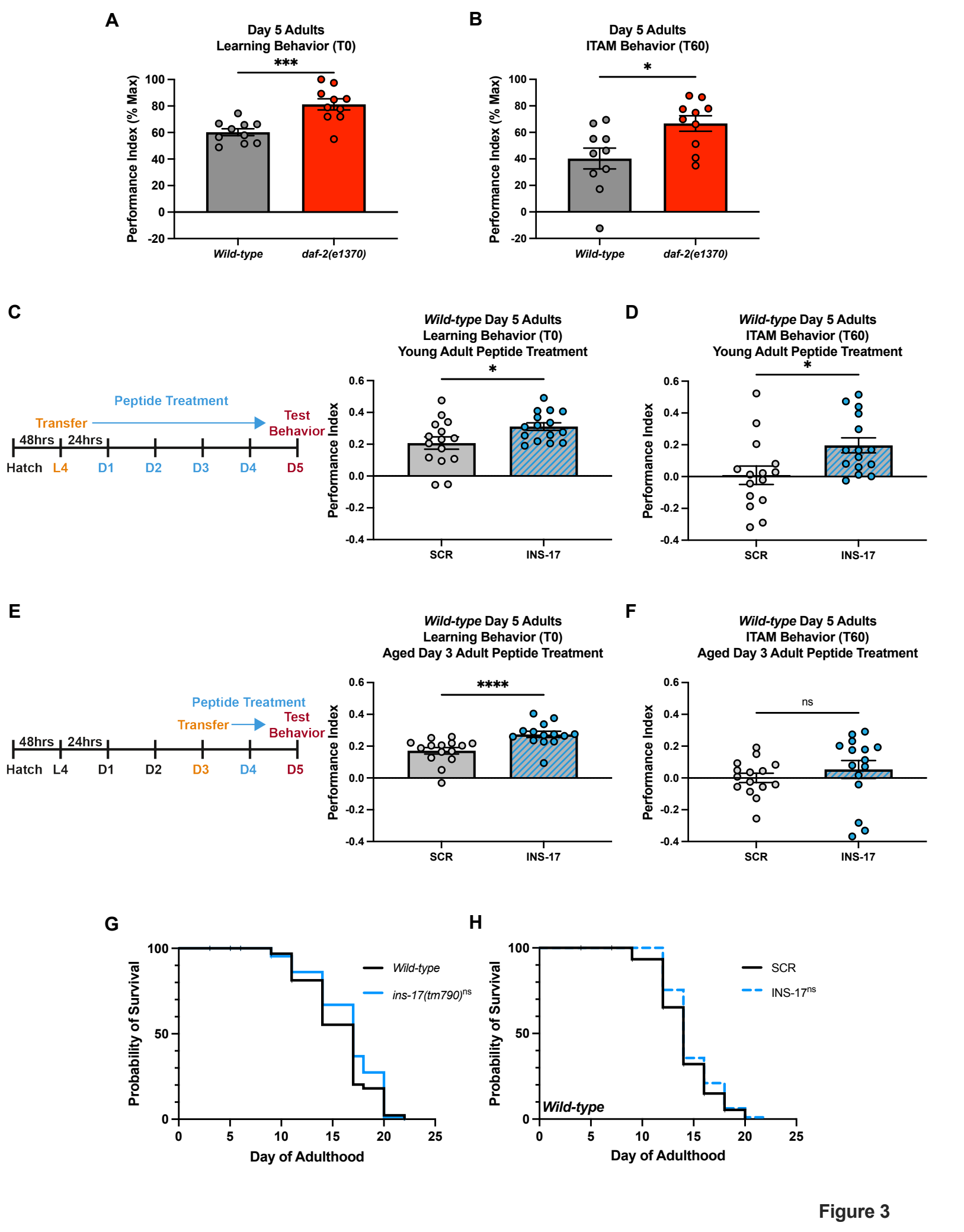
A
Day 5 Adults
Learning Behavior (T0)
***
Performance Index (% Max)
100
80
60
40
20
0
-20
Wild-type
daf-2(e1370)
B
Day 5 Adults
ITAM Behavior (T60)
*
Performance Index (% Max)
Wild-type
daf-2(e1370)
C
Peptide Treatment
Transfer
Test Behavior
48hrs
24hrs
Hatch
L4
D1
D2
D3
D4
D5
Wild-type Day 5 Adults
Learning Behavior (T0)
Young Adult Peptide Treatment
*
Performance Index
0.6
0.4
0.2
0.0
-0.2
-0.4
SCR
INS-17
D
Wild-type Day 5 Adults
ITAM Behavior (T60)
Young Adult Peptide Treatment
*
Performance Index
SCR
INS-17
E
Peptide Treatment
Transfer
Test Behavior
48hrs
24hrs
Hatch
L4
D1
D2
D3
D4
D5
Wild-type Day 5 Adults
Learning Behavior (T0)
Aged Day 3 Adult Peptide Treatment
****
Performance Index
SCR
INS-17
F
Wild-type Day 5 Adults
ITAM Behavior (T60)
Aged Day 3 Adult Peptide Treatment
ns
Performance Index
SCR
INS-17
G
Probability of Survival
100
50
0
Wild-type
ins-17(tm790)ns
0
5
10
15
20
25
Day of Adulthood
H
Probability of Survival
100
50
0
SCR
INS-17ns
Wild-type
0
5
10
15
20
25
Day of Adulthood

Figure 3

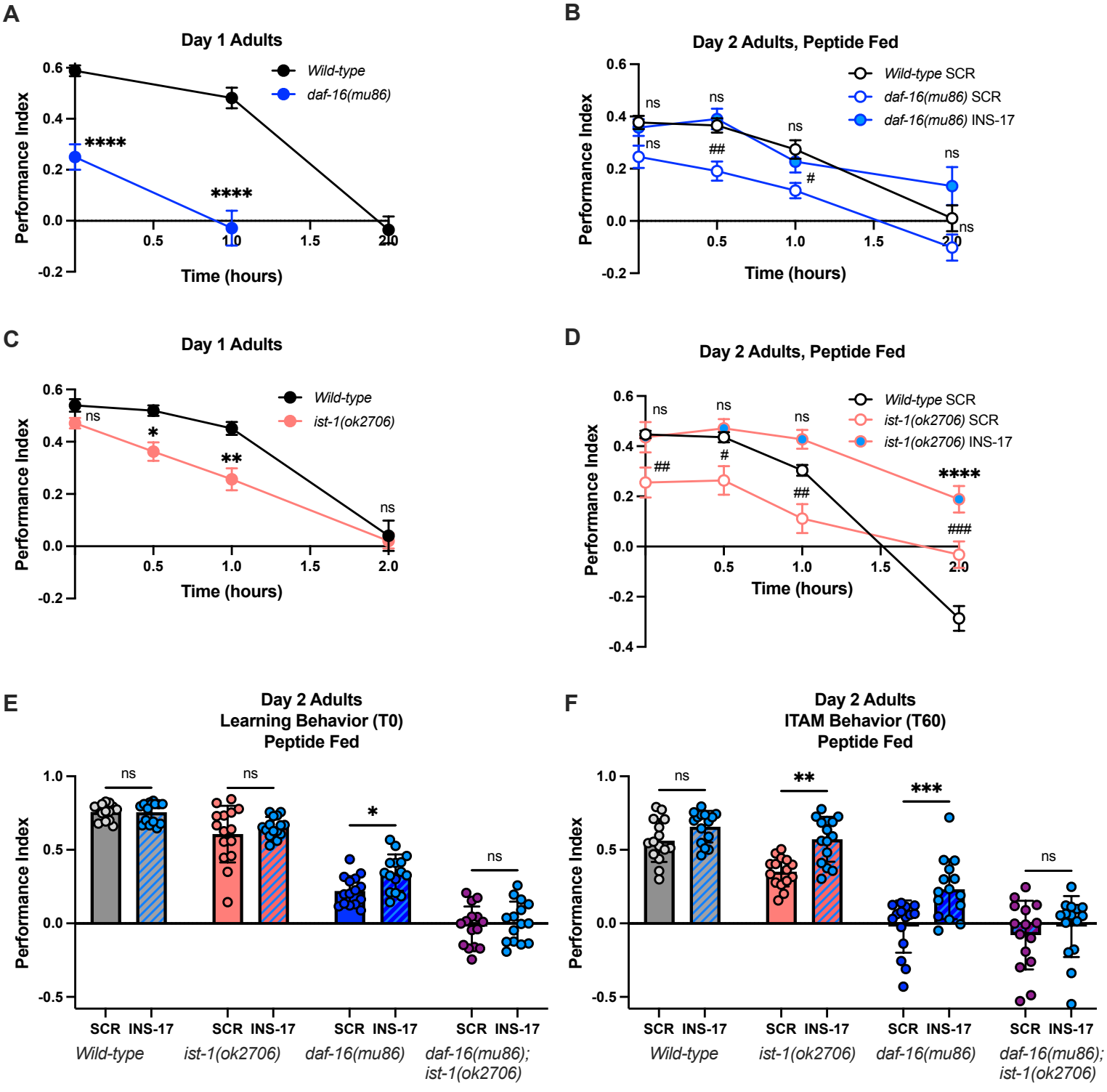
A
Day 1 Adults
Wild-type
daf-16(mu86)
Performance Index
Time (hours)
****
****
B
Day 2 Adults, Peptide Fed
Wild-type SCR
daf-16(mu86) SCR
daf-16(mu86) INS-17
Performance Index
Time (hours)
ns
ns
ns
ns
##
#
ns
ns
C
Day 1 Adults
Wild-type
ist-1(ok2706)
Performance Index
Time (hours)
ns
*
**
ns
D
Day 2 Adults, Peptide Fed
Wild-type SCR
ist-1(ok2706) SCR
ist-1(ok2706) INS-17
Performance Index
Time (hours)
ns
ns
ns
##
#
##
****
###
E
Day 2 Adults
Learning Behavior (T0)
Peptide Fed
Performance Index
ns
ns
*
ns
SCR INS-17
Wild-type
ist-1(ok2706)
daf-16(mu86)
daf-16(mu86); ist-1(ok2706)
F
Day 2 Adults
ITAM Behavior (T60)
Peptide Fed
Performance Index
ns
**
***
ns
SCR INS-17
Wild-type
ist-1(ok2706)
daf-16(mu86)
daf-16(mu86); ist-1(ok2706)

Figure 4

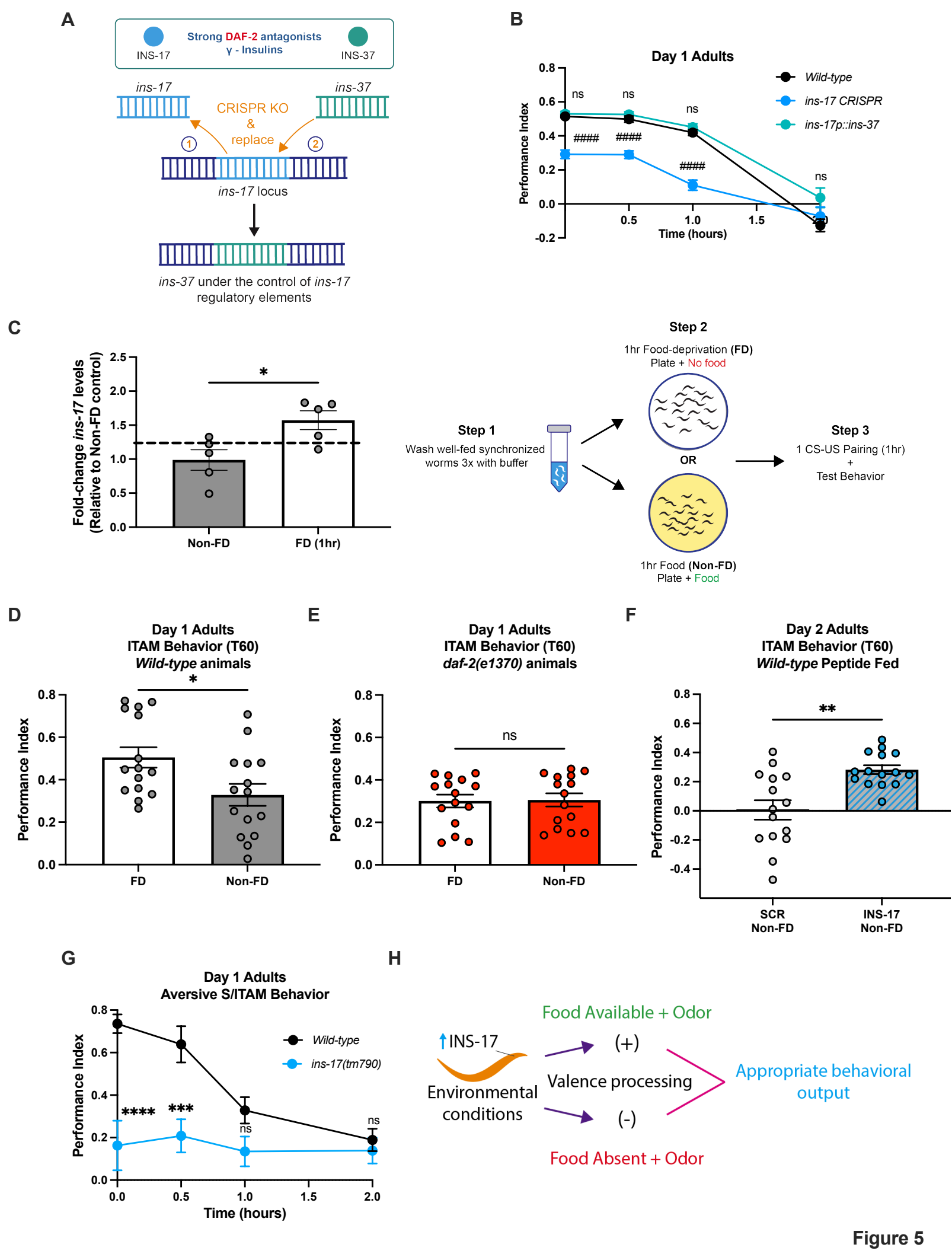
A
INS-17
Strong DAF-2 antagonists
γ - Insulins
INS-37
ins-17
ins-37
CRISPR KO
&
replace
1
2
ins-17 locus
ins-37 under the control of ins-17
regulatory elements
B
Day 1 Adults
Wild-type
ins-17 CRISPR
ins-17p::ins-37
Performance Index
Time (hours)
ns
####
C
Fold-change ins-17 levels
(Relative to Non-FD control)
Non-FD
FD (1hr)
Step 1
Wash well-fed synchronized
worms 3x with buffer
Step 2
1hr Food-deprivation (FD)
Plate + No food
OR
1hr Food (Non-FD)
Plate + Food
Step 3
1 CS-US Pairing (1hr)
+
Test Behavior
D
Day 1 Adults
ITAM Behavior (T60)
Wild-type animals
FD
Non-FD
E
Day 1 Adults
ITAM Behavior (T60)
daf-2(e1370) animals
F
Day 2 Adults
ITAM Behavior (T60)
Wild-type Peptide Fed
SCR
Non-FD
INS-17
Non-FD
G
Day 1 Adults
Aversive S/ITAM Behavior
Wild-type
ins-17(tm790)
****
***
H
INS-17
Environmental
conditions
Food Available + Odor
(+)
Valence processing
(-)
Food Absent + Odor
Appropriate behavioral
output

Figure 5